

Supporting Information for:

Tailoring Flavin-based Photosensitizers for Efficient Photooxidative Coupling of Benzylic Amines

Huimin Guo*, Yang Qiu, Siyu Liu, Xiangyu Zhang and Jianzhang Zhao

School of Chemistry, Dalian University of Technology, No. 2, Linggong Road, Dalian, 116024,
P. R. China.

Contents

1 General Information.....	S2
2 Synthesis and Molecular Structure Characterization Data.....	S4
3 Optimization of Reaction Conditions.....	S7
3 NMR and HRMS spectra.....	S9
4 DFT/TD-DFT Results.....	S40
5 References.....	S56

This file includes 1 Scheme, 87 Figures and 9 Tables within 57 pages.

KEYWORDS: Flavin; Electron Transfer; Intersystem Crossing; Photocatalysis; Photooxidation

* Corresponding authors, email: guohm@dlut.edu.cn (H.G.)

1. General Information

All the chemicals used in synthesis were of analytical purity and were used as received. Solvents were dried and distilled before used for synthesis.

Analytical Measurements. All chemicals are analytically pure and used as received. NMR spectra were recorded on a Bruker 400 MHz spectrometer with CDCl_3 , $\text{DMSO}-d_6$ as solvents and tetramethylsilane (TMS) as standard at 0.00 ppm. HRMS were measured with a G6224A (Agilent, U.S.).

Spectroscopic Measurements. Absorption spectrum were recorded on an UV2550 UV–Vis spectrophotometer (Shimadzu, Japan). Fluorescence spectra were measured on an FS5 spectrophotometer (Edinburgh Instruments, UK). Fluorescence lifetimes were measured with an OB920 luminescence lifetime spectrometer (Edinburgh Instruments, UK). The nanosecond transient absorption spectra were measured on LP920 laser flash photolysis spectrometer (Edinburgh Instruments Ltd., UK). Luminescence Quantum Yield were measured with an C13534-11 Quantaurus-QY Plus (Hamamatsu Photonics, Japan).

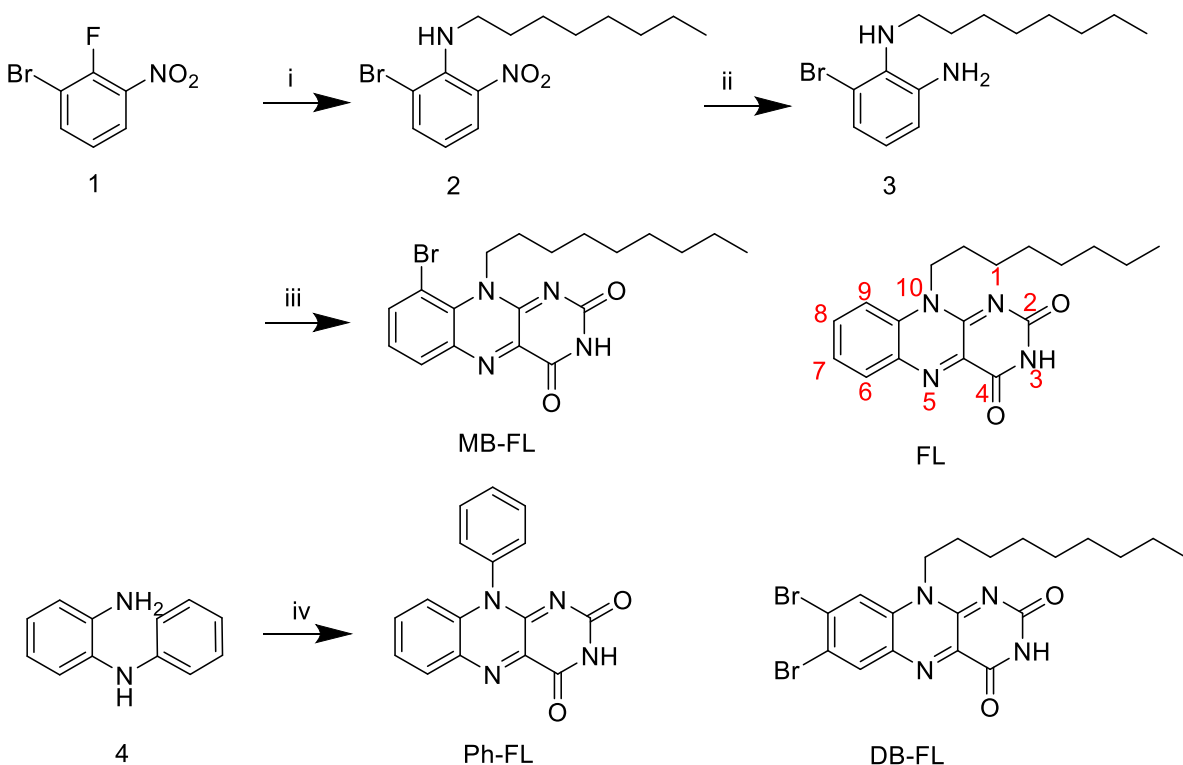
Preparation of Sample Solution for Spectroscopic Measurements. The compound was dissolved in a small amount of solvent in a 5 mL volumetric flask and then toluene was added to get 5 mL solution (1.0×10^{-3} M).

Singlet Oxygen Quantum Yield (Φ_Δ). 1,3-Diphenylisobenzofuran (DPBF) was used as ${}^1\text{O}_2$ scavenger and the ${}^1\text{O}_2$ production was monitored by following the absorbance of DPBF at 414 nm. A comparative method was used and was calculated according to the following equation (1) to determine the singlet oxygen quantum yield.

$$\Phi_{\Delta,\text{nuk}} = \Phi_{\Delta,\text{std}} \left(\frac{A_{\text{std}}}{A_{\text{nuk}}} \right) \left(\frac{I_{\text{unk}}}{I_{\text{std}}} \right) \left(\frac{\eta_{\text{unk}}}{\eta_{\text{std}}} \right)^2 \quad (1)$$

In the above equation, unk and std indicate the unknown sample and the standard, respectively. Φ , A , m , and η represent the singlet oxygen quantum yield, absorbance at excitation wavelength, slope of the absorbance of DPBF changing over time, and refractive index of the solvent used for measurement, respectively. Optically matched solutions were used (the solutions of the sample and the standard should give the same absorbance at the excitation wavelength). Anthracene was used as standard ($\Phi_{\Delta} = 0.60$ in CH₃CN).

2. Synthesis and Molecular Structure Characterization Data



Scheme S1. Synthesis of the compounds. Reaction conditions: (i) Octyl amine, THF, 66 °C, 16 h ; (ii) Zn, NH₄Cl, CH₃OH/H₂O, 45 °C, 24 h ; (iii) Alloxan, boric acid,acetic acid glacial, 70 °C, 3 h ; (iv) Alloxan, boric acid, acetic acid glacial,25 °C, 12 h .

Synthesis of the compound 2: Compound 1 (219 mg, 1 mmol) was dissolved in a round-bottomed flask of tetrahydrofuran THF (40 ml). *N*-octylamine (1.2 ml, 6 mmol) and triethylamine (0.3 ml) were added with a syringe under nitrogen atmosphere. The reaction mixture was stirred at 66 °C for 16 h. At the end of the reaction, the crude product was purified by vacuum concentration and silica gel chromatography. The eluent was dichloromethane methane and petroleum ether (v/v=1:3), and the orange-yellow product 2 was obtained with the weight of 312 mg and the yield of 95.2%. ¹H NMR (400 MHz, CDCl₃) : δ 0.85-0.95 (m, 3 H), 1.22-1.42(m, 11 H), 1.57-1.69 (m, 2 H), 3.28 (2 H, t, J = 7.07 Hz), 6.70 (t, J = 8.07 Hz, 1 H), 7.70 (dd, J = 7.75, 1.50 Hz, 1 H), 7.90 (dd, J=8.38, 1.50 Hz, 1 H).

Synthesis of the compound MB-FL: Compound 2 (275.5 mg, 0.84 mmol) was dissolved in a mixture of methanol-water (v/v=2:1), and zinc powder (274 mg, 4.2 mmol) and NH₄Cl (456 mg, 8.2 mmol) were slowly added under the conditions of ice bath and nitrogen. The reaction was placed under 45 °C and nitrogen atmosphere for 24 h. The insoluble impurities were removed by vacuum filtration at the end of the reaction, and the pH of the solution was adjusted to neutral using NaHCO₃. Dichloromethane is then used for extraction and decompression concentration to obtain crude product 3.

The crude product 3 (100 mg), boric acid (21.3 mg) and alloxouracil (60.6 mg) were dissolved in an appropriate amount of glacial acetic acid and stirred for 3 h at 70 °C. At the end of the reaction, the insoluble impurities are removed by filtration to obtain the crude product. The glacial acetic acid in the crude product was removed using a rotary evaporator and dichloromethane was added. The crude product was purified by silica gel chromatography. The eluent was dichloromethane and methanol (v/v=40:1), and the orange product was 49 mg (yield 36%). ¹H NMR (400 MHz, DMSO-d₆) : δ 0.84-0.88 (m, 3 H), 1.27 (br. S., 10 H), 1.88 (br. S., 2 H), 4.86 (br. S., 2 H), 7.51 (t, J = 7.88 Hz, 1 H), 8.13 (d, J = 8.00 Hz, 1 H), 8.24 (d, J = 7.63 Hz, 1 H), 11.52 (s, 1 H). ¹³C NMR (101 MHz, DMSO-d₆) : δ 14.40 (s, 1 C), 22.53 (s, 1 C), 26.28 (s, 1 C), 28.64 (s, 1 C), 29.01 (s, 1 C), 29.12 (s, 1 C), 31.64 (s, 1 C), 48.06 (s, 1 C), 107.47 (s, 1 C), 127.12 (s, 1 C), 132.44 (s, 1 C), 133.32 (s, 1 C), 137.69 (s, 1 C), 139.40 (s, 1 C), 142.52 (s, 1 C), 152.58 (s, 1 C), 156.06 (s, 1 C), 159.89 (s, 1 C). ESI-TOF-HRMS ([C₁₈H₂₁BrN₄O₂+H]⁺) : Calculated value 405.0926, experimental value 405.0917.

Synthesis of the compound Ph-FL: The crude product 4 (50 mg), boric acid (21.3 mg) and alloxouracil (60.6 mg) were dissolved in an appropriate amount of glacial acetic acid and stirred overnight at room temperature and pressure. At the end of the reaction, the insoluble impurities

are removed by filtration to obtain the crude product. The glacial acetic acid in the crude product was removed by a rotary evaporator and dichloromethane was added. The crude product was purified by silica gel chromatography. The eluent was dichloromethane methane and methanol (v/v=40:1) to obtain a bright yellow product of 70.9 mg (90% yield). ¹H NMR (400 MHz, DMSO-d₆) : δ 6.76 (d, J = 8.25 Hz, 1 H), 7.44 (d, J = 7.25 Hz, 2 H), 7.61 7.77 (m, 6 H), 8.20 (dd, J = 8.13, 1.25 Hz, 1 H), 11.42 (s, 1 H). ¹³C NMR (101 MHz, DMSO-d₆) : δ 14.40 (s, 1 C), 22.53 (s, 1 C), 26.28 (s, 1 C), 28.64 (s, 1 C), 29.01 (s, 1 C), 29.12 (s, 1 C), 31.64 (s, 1 C), 48.06 (s, 1 C), 107.47 (s, 1 C), 127.12 (s, 1 C), 132.44 (s, 1 C), 133.32 (s, 1 C), 137.69 (s, 1 C), 139.40 (s, 1 C), 142.52 (s, 1 C), 152.58 (s, 1 C), 156.06 (s, 1 C), 159.89 (s, 1 C). ESI-TOF-HRMS ([C₁₆H₁₀N₄O₂-H]⁻) : Calculated value 289.0726, experimental value 289.0732.

3. Optimization of Reaction Conditions

Table S3-1 Optimization of reaction conditions for MB-FL sensitized photooxidative coupling of benzylamines for synthesis of imines.^{a,b}

Entry	Sensitizer	Sensitizer Concentration (mol %)	Duration (h)	Solvent	Yield (%)
1	MB-FL	0.5	9	DCM	42
2	MB-FL	0.5	9	MeCN	75
3	MB-FL	0.5	9	MeOH	40
4	MB-FL	0.5	9	MeCN:MeOH	67
5	MB-FL	0.5	9	MeCN:H ₂ O	86
6	MB-FL	0.5	3	MeCN:H ₂ O	63
7	MB-FL	0.5	5	MeCN:H ₂ O	76
8	MB-FL	0.5	7	MeCN:H ₂ O	80
9	MB-FL	0.5	11	MeCN:H ₂ O	90
10	None	None	9	MeCN:H ₂ O	0
11	MB-FL	0.5	9	MeCN:H ₂ O, No light	0
12	MB-FL	0.5	9	MeCN:H ₂ O, No O ₂	0

^a Benzylamine (0.2 mmol) as substrate, the light wavelength was 451 nm, the light intensity was 1400 W/m². Further experimental details and ¹H-NMR of product mixtures were included in the Supporting Information. ^b The composition of mixed MeCN /MeOH, DCM/MeOH and MeCN /H₂O solvents are v:v = 9:1, otherwise specified.

Table S3-2 Optimization of reaction conditions for Ph-FL sensitized photooxidative coupling of benzyl amines for synthesis of imines.^{a,b}

Entry	Sensitizer	Sensitizer Concentration (mol %)	Duration (h)	Solvent	Yield (%)
1	Ph -FL	0.5	9	MeOH	8
2	Ph -FL	0.5	9	MeCN	53
3	Ph -FL	0.5	9	DCM	26
4	Ph -FL	0.5	9	MeCN:MeOH	28
5	Ph -FL	0.5	9	MeCN:H ₂ O	14
6	Ph -FL	0.5	3	MeCN	35
7	Ph -FL	0.5	5	MeCN	40
8	Ph -FL	0.5	7	MeCN	44
9	Ph -FL	0.5	11	MeCN	58
10	None	None	9	MeCN	0
11	Ph -FL	0.5	9	MeCN, No light	0
12	Ph -FL	0.5	9	MeCN, No O ₂	0

^a Benzylamine (0.2 mmol) as substrate, the light wavelength was 451 nm, the light intensity was 1400 W/m². Further experimental details and ¹H-NMR of product mixtures were included in the Supporting Information. ^b The composition of mixed MeCN /MeOH and MeCN /H₂O solvents are v:v = 9:1, unless specified explicitly.

4. NMR and HRMS spectra

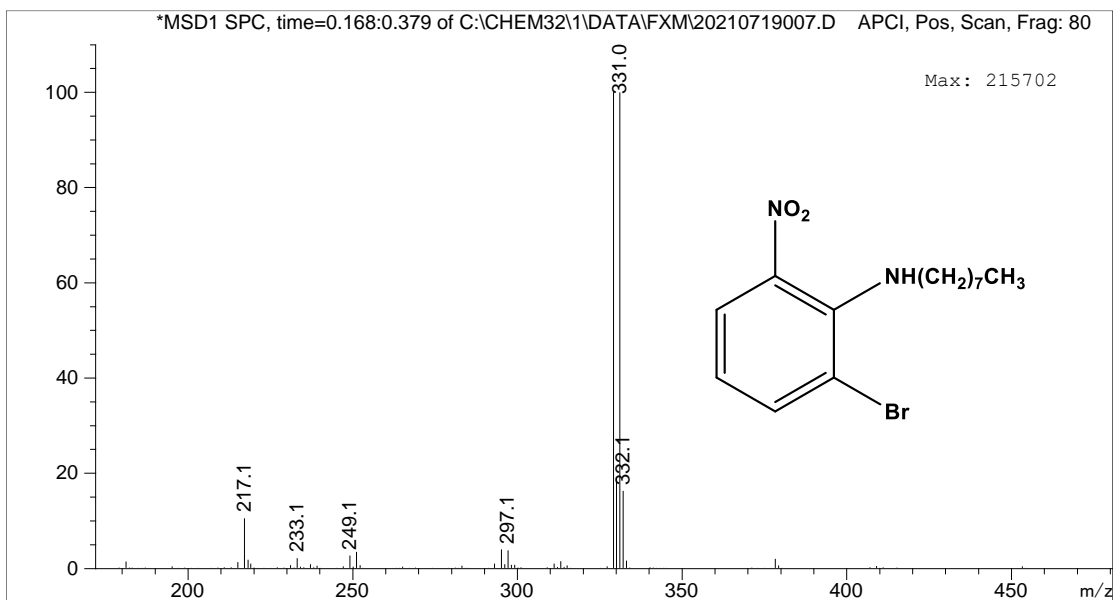


Figure S4-1. MS spectrum of **2**.

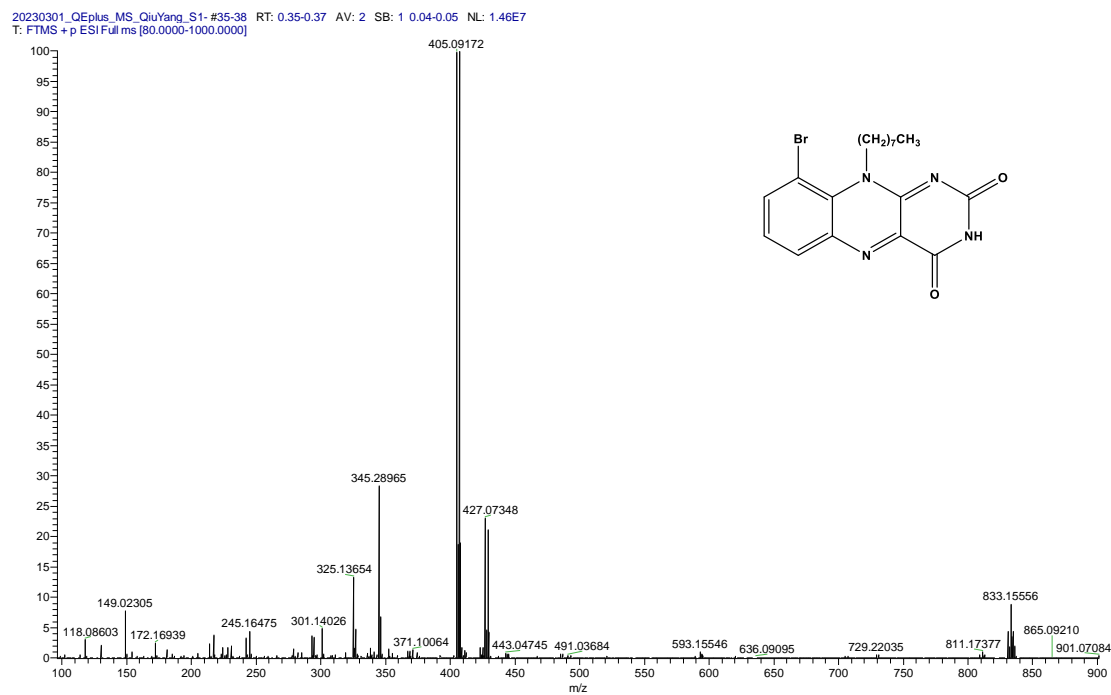


Figure S4-2. HRMS spectrum of **MB-FL**.

20230221_QEplus_MS_Qiuyang_S1 #19 RT: 0.20 AV: 1 SB: 2 0.06-0.08 NL: 1.51E0
T: FTMS - p ESI Full ms [80.0000-1000.0000]

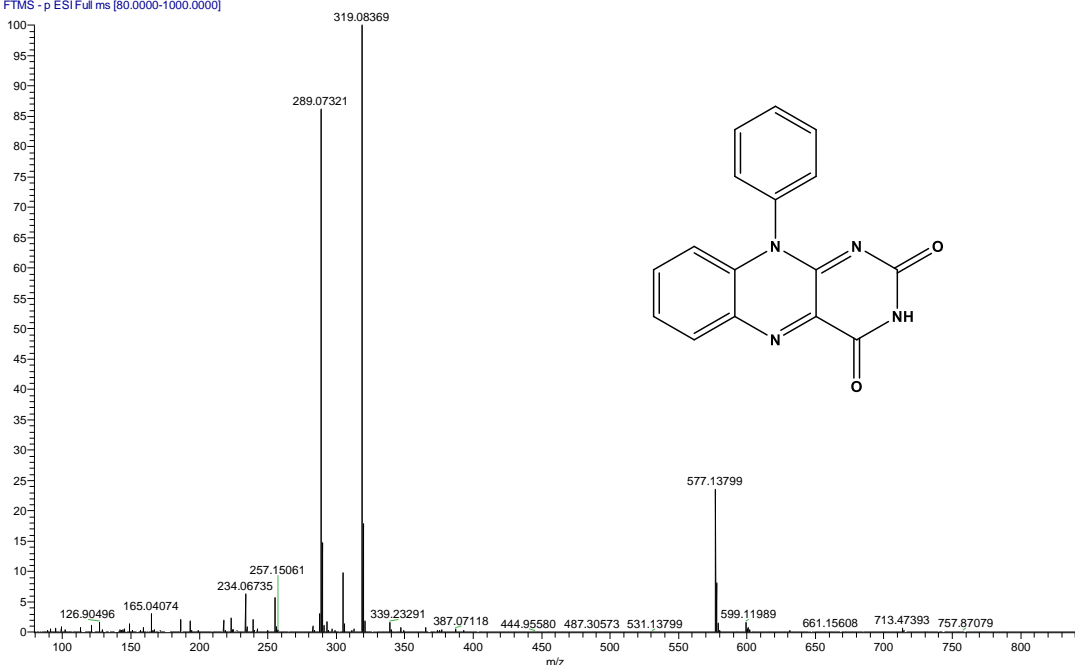


Figure S4-3. HRMS spectrum of **Ph-FL**.

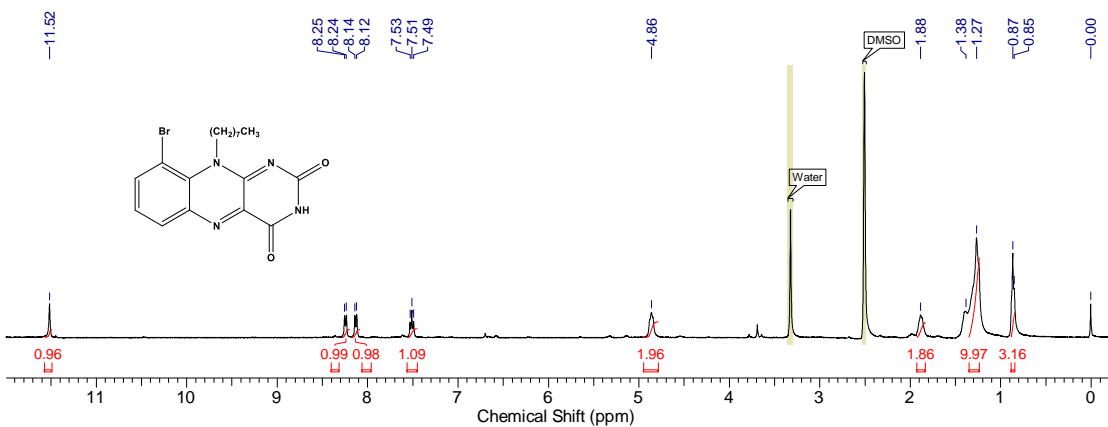


Figure S4-4. ^1H NMR spectrum of **MB-FL** (400 MHz, $\text{DMSO}-d_6$), 25 °C.

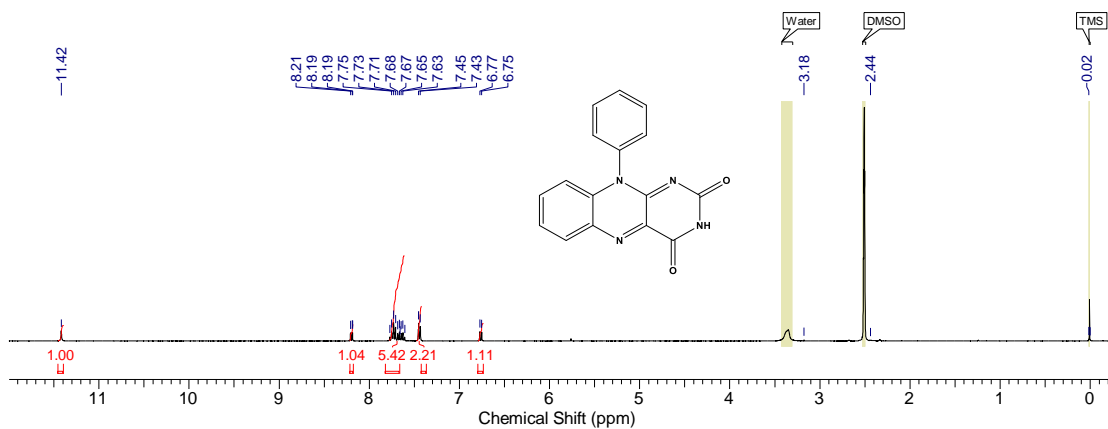


Figure S4-5. ¹H NMR spectrum of **Ph-FL** (400 MHz, DMSO-*d*₆), 25 °C.

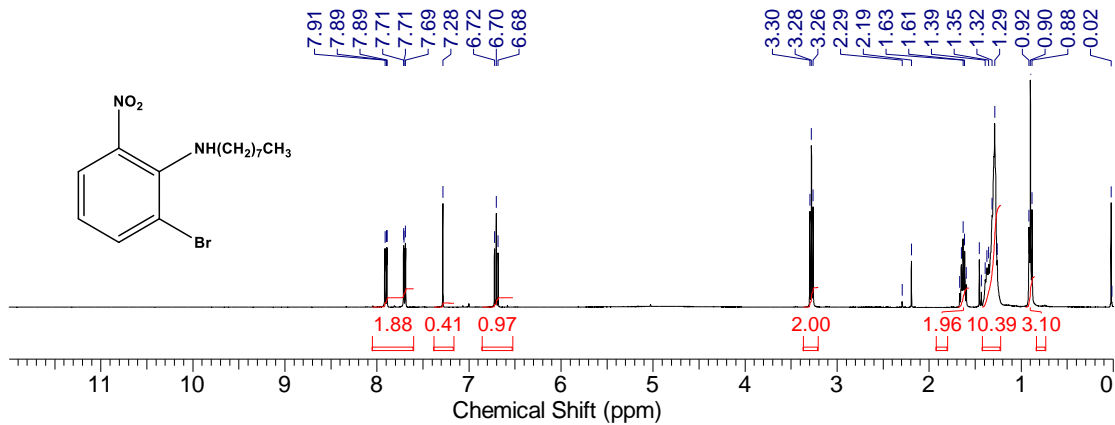


Figure S4-6. ¹H NMR spectrum of **2** (400 MHz, CDCl₃), 25 °C.

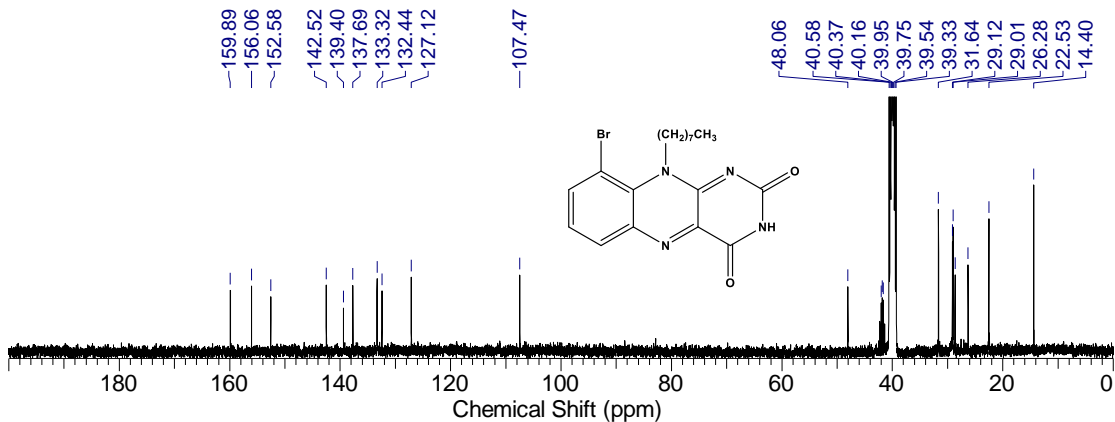


Figure S4-7. ¹³C NMR spectrum of **2** (101 MHz, DMSO-*d*₆), 25 °C.

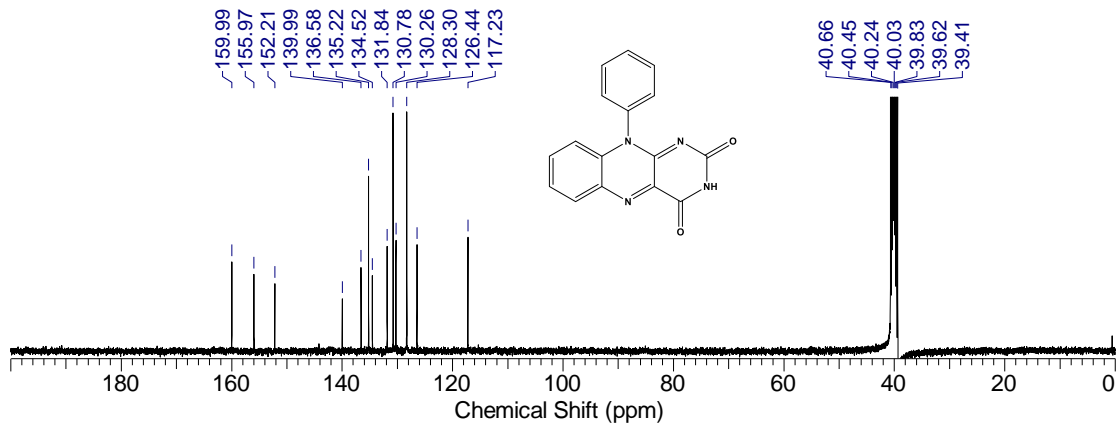


Figure S4-8. ^{13}C NMR spectrum of **2** (101 MHz, $\text{DMSO}-d_6$), 25 °C.

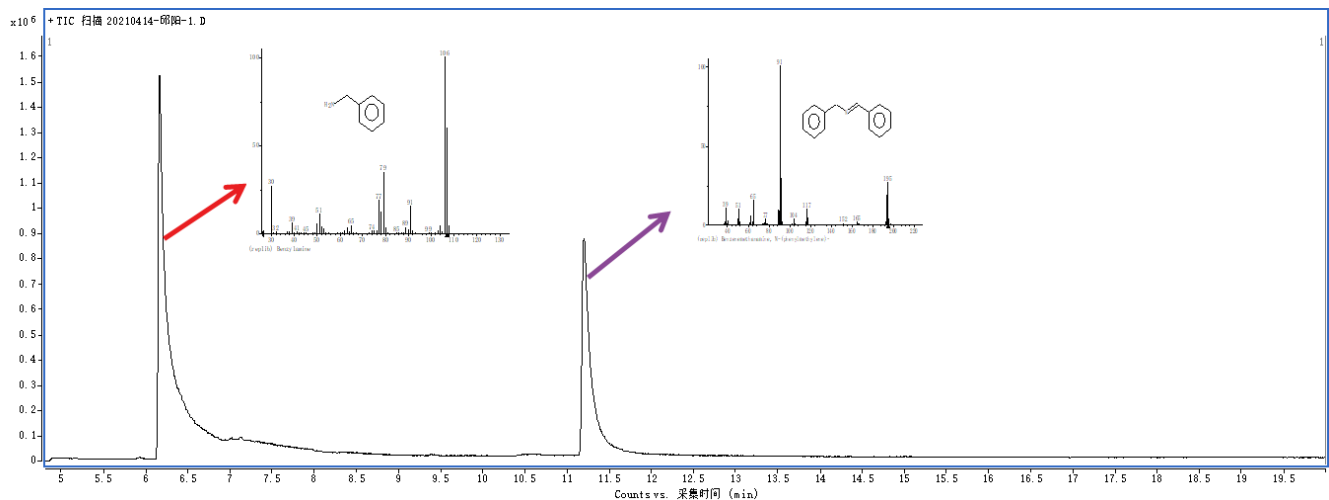


Figure S4-9. GC-MS spectra of benzylamine catalyzed by FL photocatalysis.

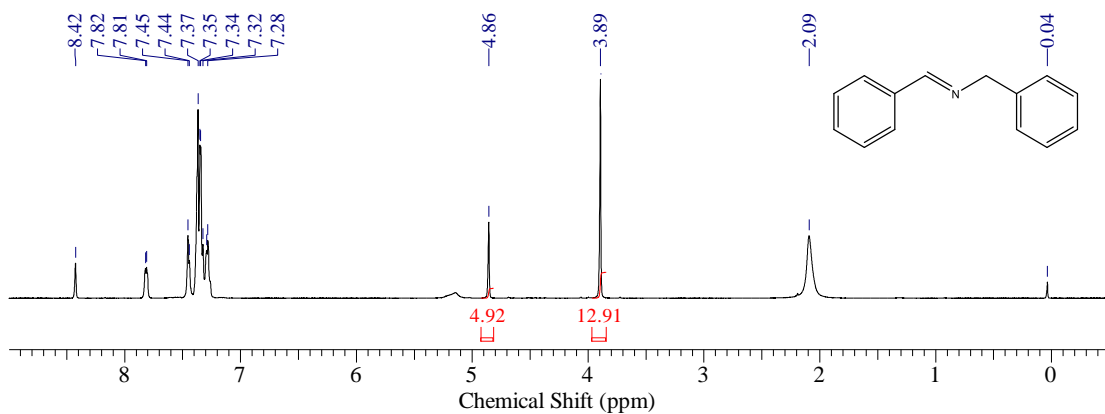


Figure S4-10. ^1H NMR(CDCl_3 , 400 MHz), Photosensitizer:FL(0.2 mol%), Reaction solvent: CH_3CN , Reaction time:9 h, Yield:43 %.

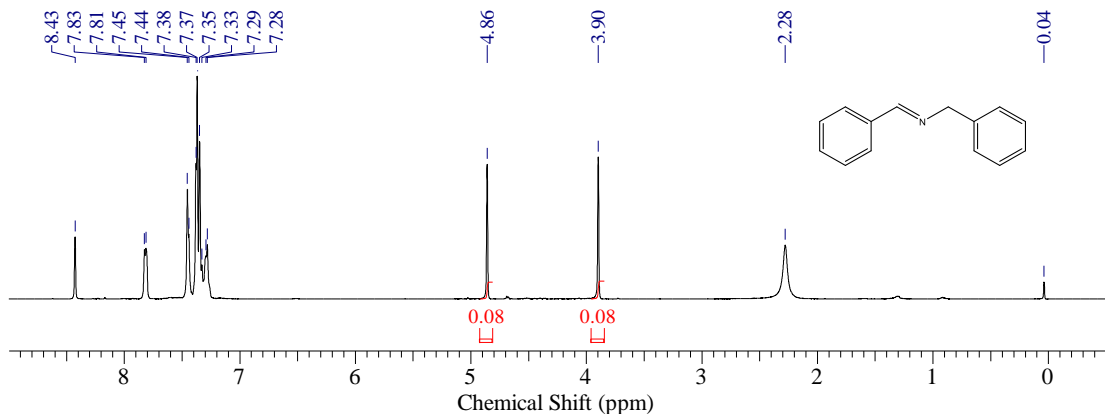


Figure S4-11. ^1H NMR(CDCl_3 , 400MHz), Photosensitizer:FL(0.5 mol%), Reaction solvent: CH_3CN , Reaction time:9 h, Yield: 67 %.

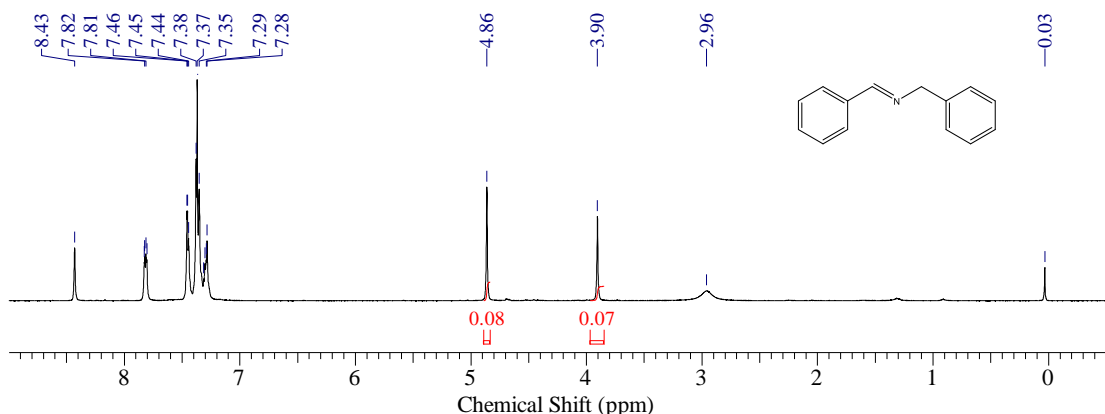


Figure S4-12. ^1H NMR(CDCl_3 , 400 MHz), Photosensitizer: FL(1 mol%), Reaction solvent: CH_3CN , Reaction time: 9 h, Yield: 70 %.

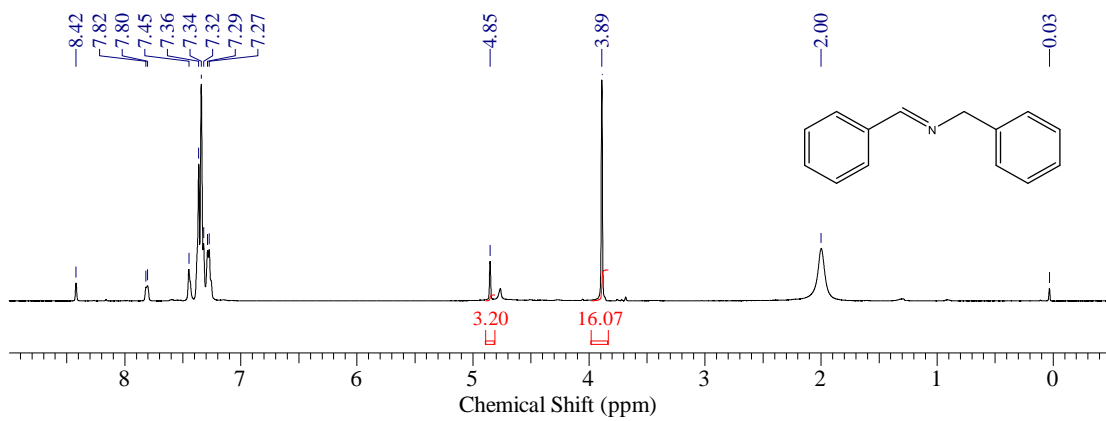


Figure S4-13. ^1H NMR(CDCl_3 , 400 MHz), Photosensitizer:FL(0.5 mol%), Reaction solvent: CH_3OH , Reaction time: 9 h, Yield: 30 %.

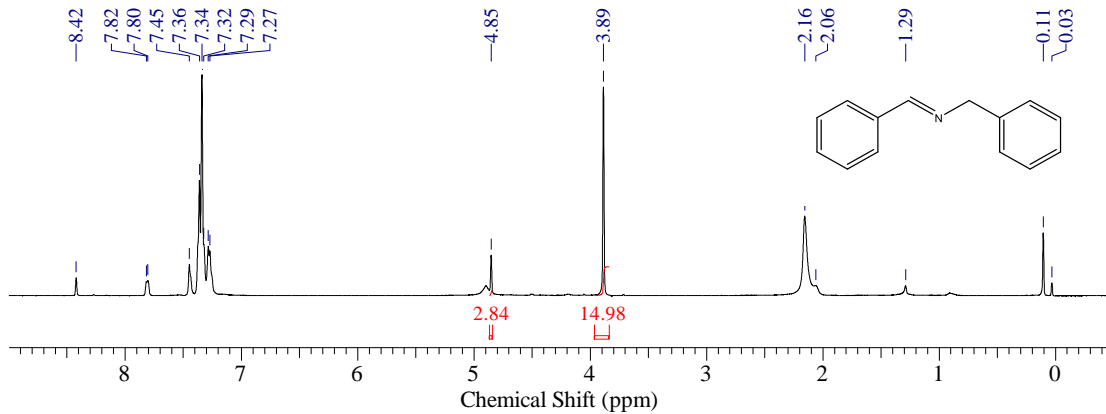


Figure S4-14. ^1H NMR(CDCl_3 , 400 MHz), Photosensitizer:FL(0.5 mol%), Reaction solvent: CH_2Cl_2 , Reaction time: 9 h, Yield: 24 %.

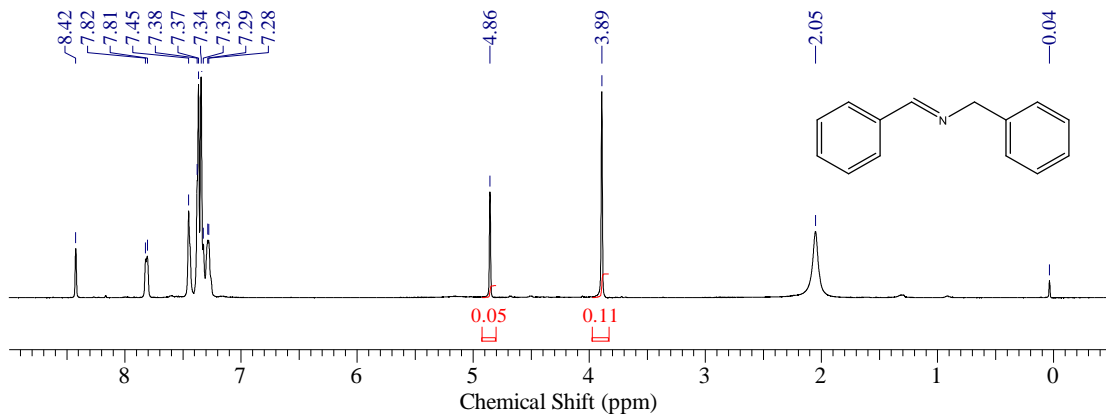


Figure S4-15. ^1H NMR(CDCl_3 , 400 MHz), Photosensitizer: FL(0.5 mol%), Reaction solvent: $\text{CH}_3\text{CN} : \text{CH}_3\text{OH} = 9:1$ (v:v), Reaction time: 9 h, Yield: 48 %.

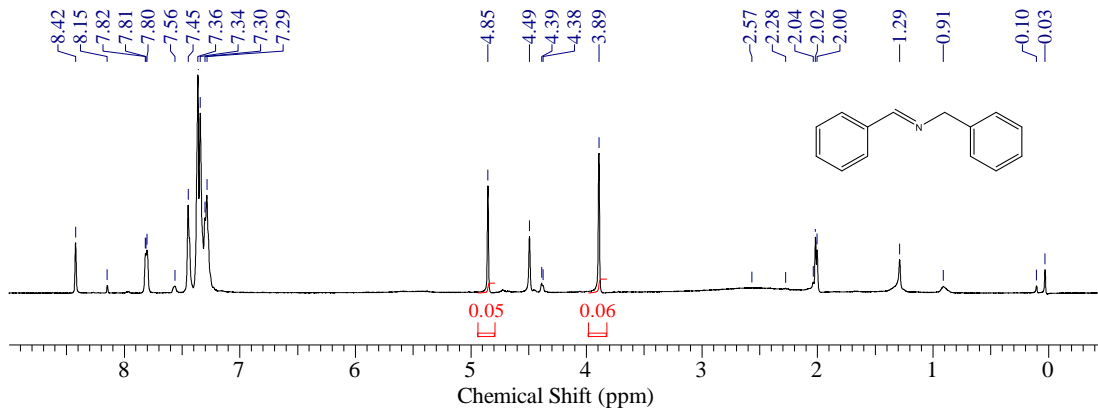


Figure S4-16. ^1H NMR(CDCl_3 , 400 MHz), Photosensitizer:FL(0.5 mol%), Reaction solvent: $\text{CH}_3\text{CN}:\text{H}_2\text{O} = 9:1$ (v:v), Reaction time: 9 h, Yield: 63 %.

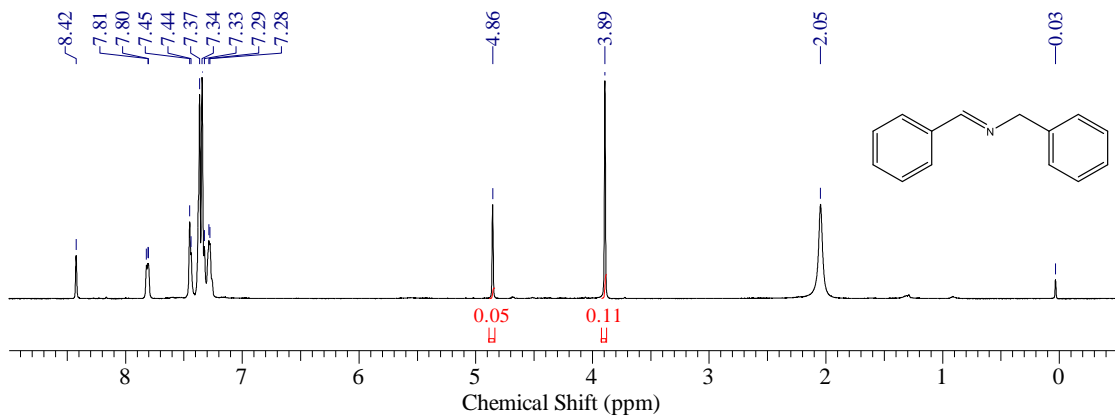


Figure S4-17. ^1H NMR(CDCl_3 , 400 MHz), Photosensitizer: FL(0.5 mol%), Reaction solvent: CH_3CN , Reaction time: 3 h, Yield: 48 %.

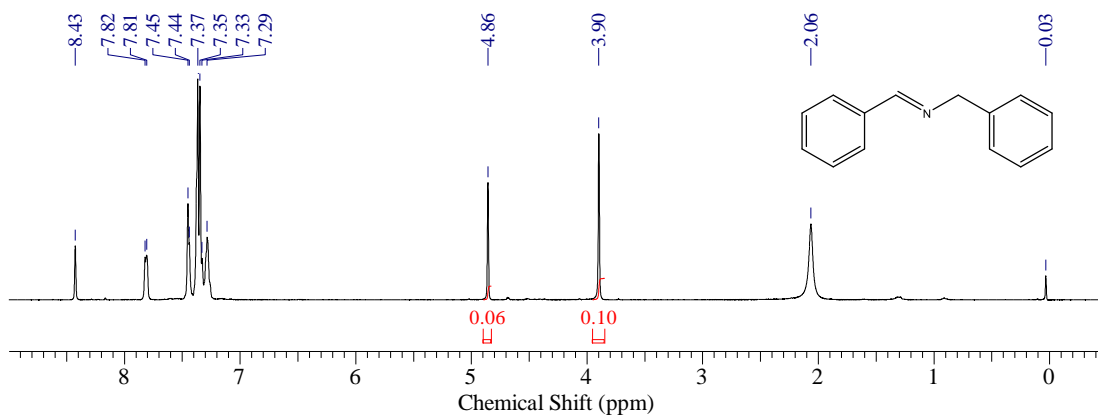


Figure S4-18. ^1H NMR(CDCl_3 , 400 MHz), Photosensitizer:FL(0.5 mol%), Reaction solvent: CH_3CN , Reaction time: 5 h, Yield: 55 %.

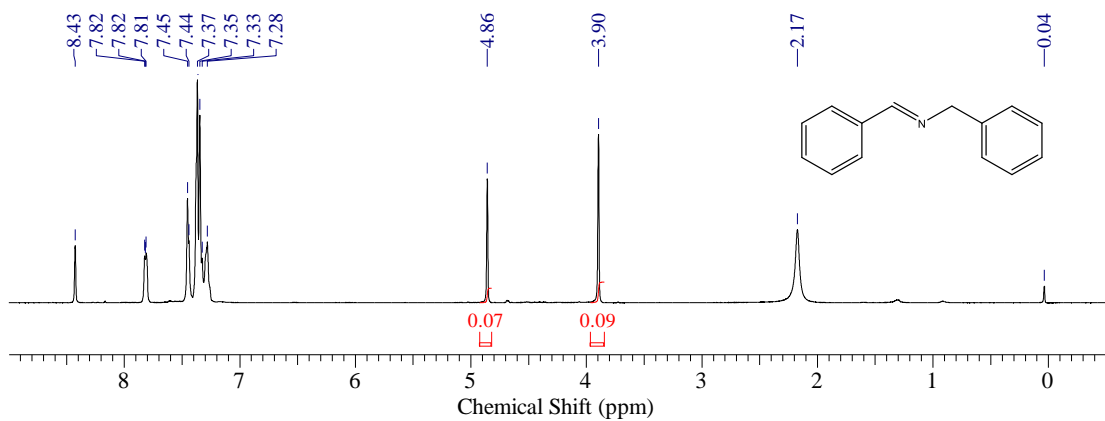


Figure S4-19. ^1H NMR(CDCl_3 , 400 MHz), Photosensitizer: FL(0.5 mol%), Reaction solvent: CH_3CN , Reaction time: 7 h, Yield: 61 %.

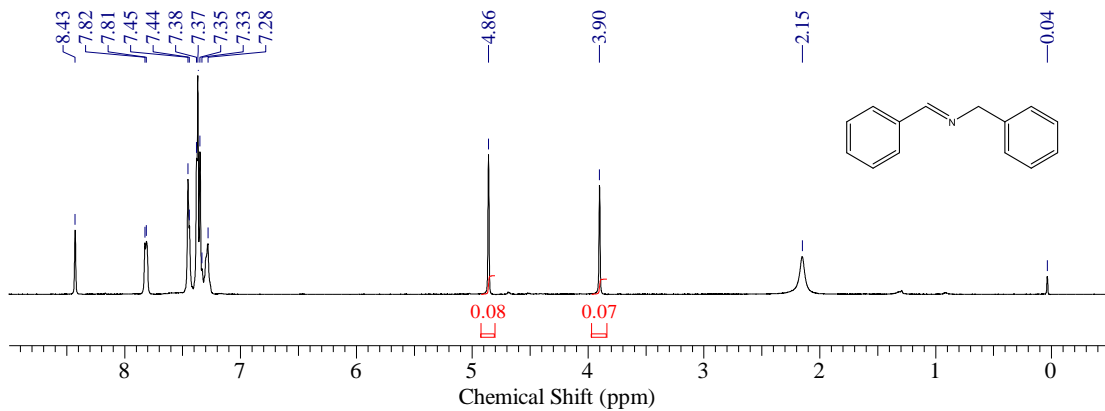


Figure S4-20. ^1H NMR(CDCl_3 , 400 MHz), Photosensitizer: FL(0.5 mol%), Reaction solvent: CH_3CN , Reaction time: 11 h, Yield: 70 %.

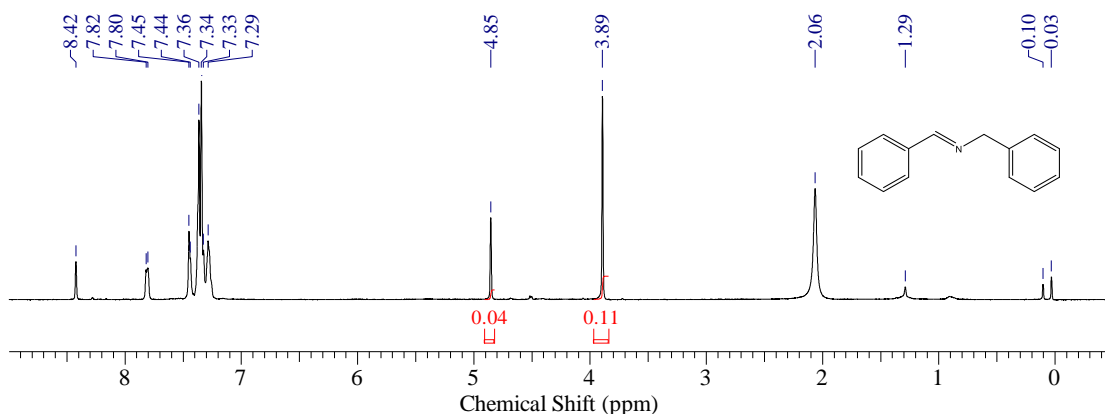


Figure S4-21. ^1H NMR(CDCl_3 , 400 MHz), Photosensitizer: MB-FL (0.5 mol%), Reaction solvent: CH_2Cl_2 , Reaction time: 9 h, Yield: 42 %.

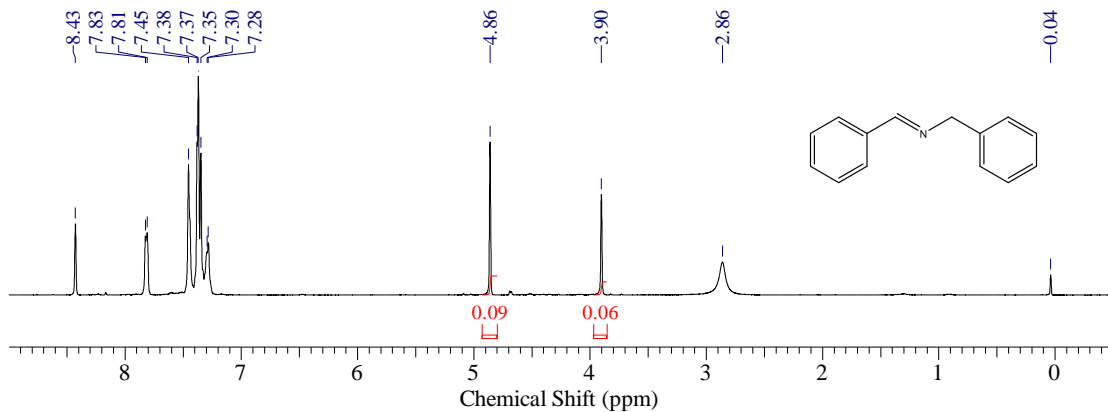


Figure S4-22. ^1H NMR(CDCl_3 , 400 MHz), Photosensitizer: MB-FL (0.5 mol%), Reaction solvent: CH_3CN , Reaction time: 9 h, Yield: 75 %.

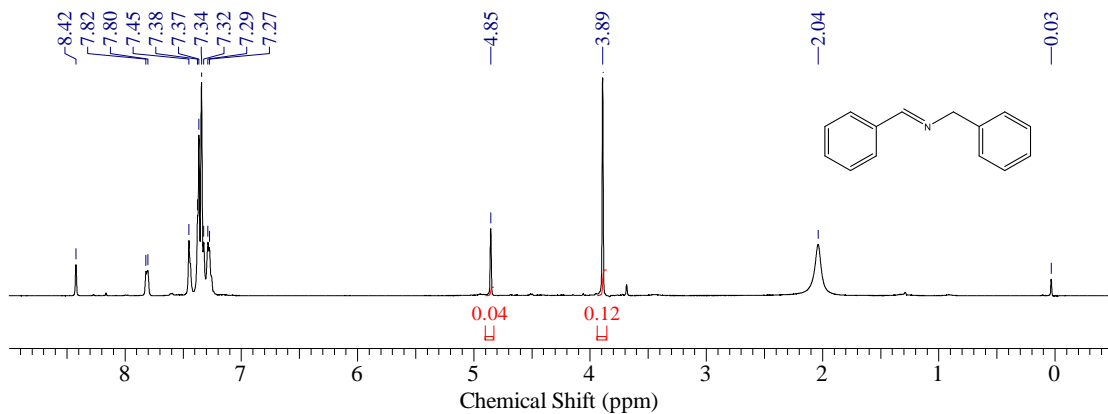


Figure S4-23. ^1H NMR(CDCl_3 , 400 MHz), Photosensitizer: MB-FL (0.5 mol%), Reaction solvent: CH_3OH , Reaction time: 9 h, Yield: 40 %.

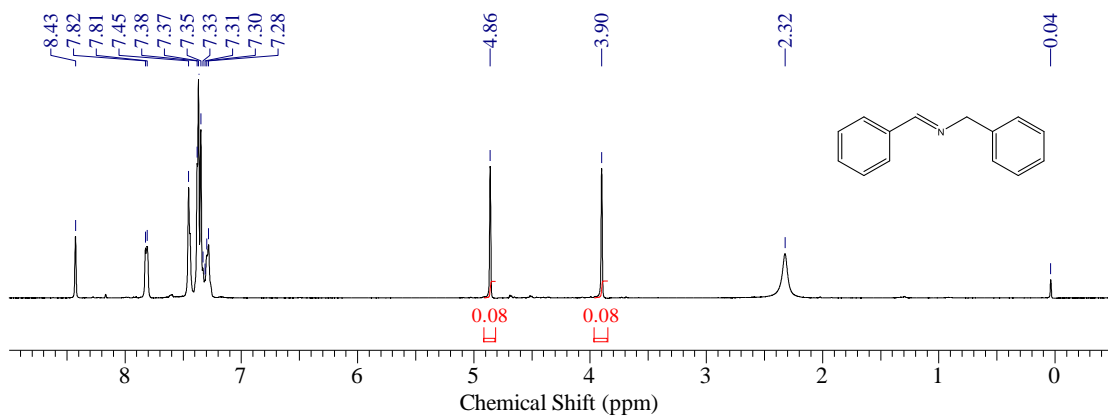


Figure S4-24. ^1H NMR(CDCl_3 , 400 MHz), Photosensitizer: MB-FL (0.5 mol%), Reaction solvent: CH_3CN : CH_3OH = 9:1(v:v), Reaction time: 9 h, Yield: 67 %.

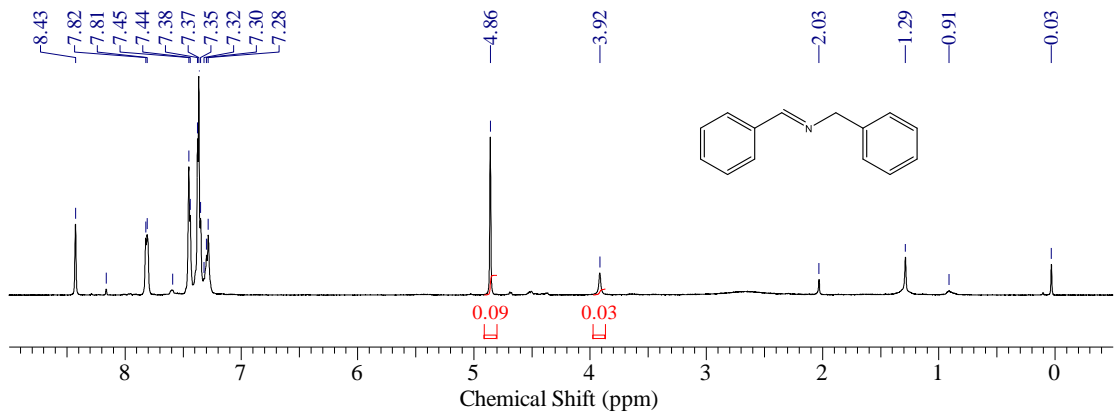


Figure S4-25. ^1H NMR(CDCl_3 , 400 MHz), Photosensitizer: MB-FL (0.5 mol%), Reaction solvent: $\text{CH}_3\text{CN}:\text{H}_2\text{O} = 9:1$ (v:v), Reaction time: 9 h, Yield: 86 %.

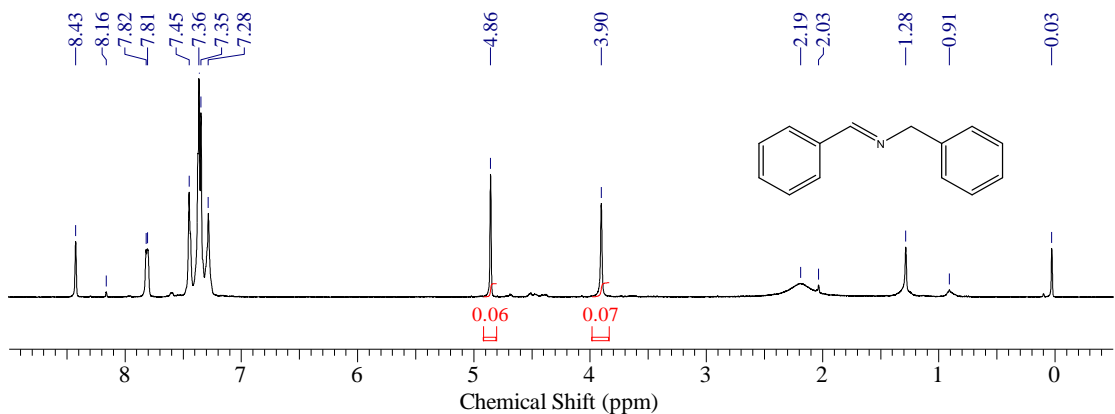


Figure S4-26. ^1H NMR(CDCl_3 , 400 MHz), Photosensitizer: MB-FL (0.5 mol%), Reaction solvent: $\text{CH}_3\text{CN}:\text{H}_2\text{O} = 9:1$ (v:v), Reaction time: 3 h, Yield: 63 %.

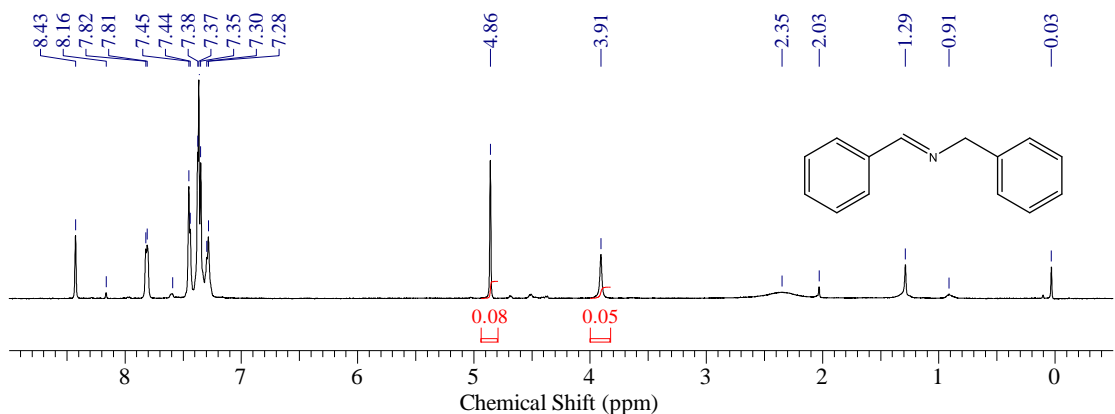


Figure S4-27. ^1H NMR(CDCl_3 , 400 MHz), Photosensitizer: MB-FL (0.5 mol%), Reaction solvent: $\text{CH}_3\text{CN}:\text{H}_2\text{O} = 9:1$ (v:v), Reaction time: 5 h, Yield: 76 %.

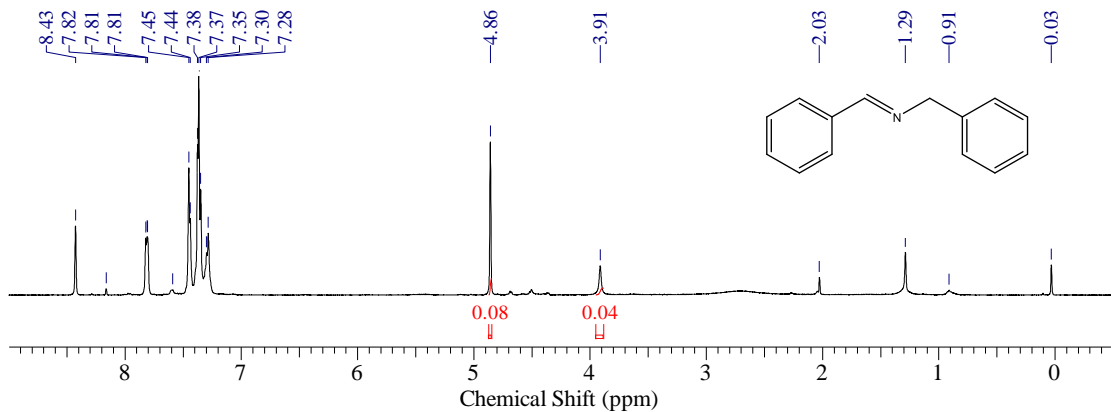


Figure S4-28. ^1H NMR(CDCl_3 , 400 MHz), Photosensitizer: MB-FL (0.5 mol%), Reaction solvent: $\text{CH}_3\text{CN} : \text{H}_2\text{O} = 9:1$ (v:v), Reaction time: 7 h, Yield: 80 %.

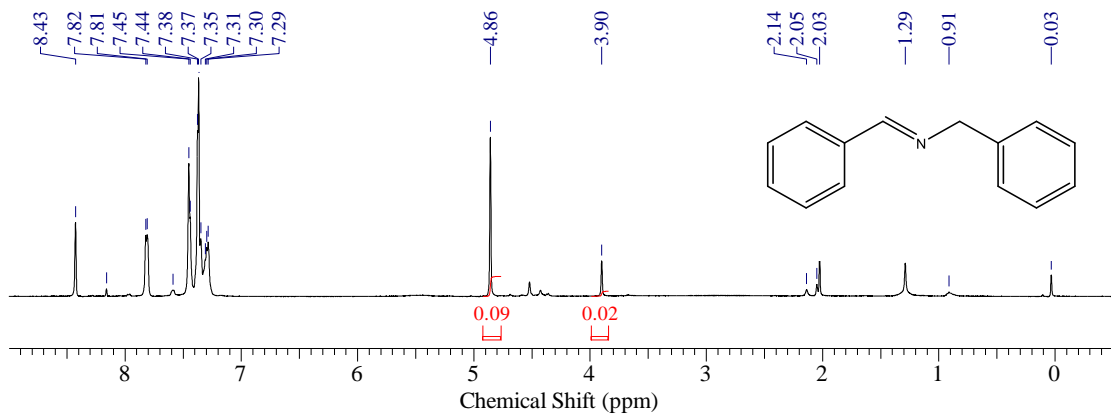


Figure S4-29. ^1H NMR(CDCl_3 , 400 MHz), Photosensitizer: MB-FL (0.5 mol%), Reaction solvent: $\text{CH}_3\text{CN} : \text{H}_2\text{O} = 9:1$ (v:v), Reaction time: 11 h, Yield: 90 %.

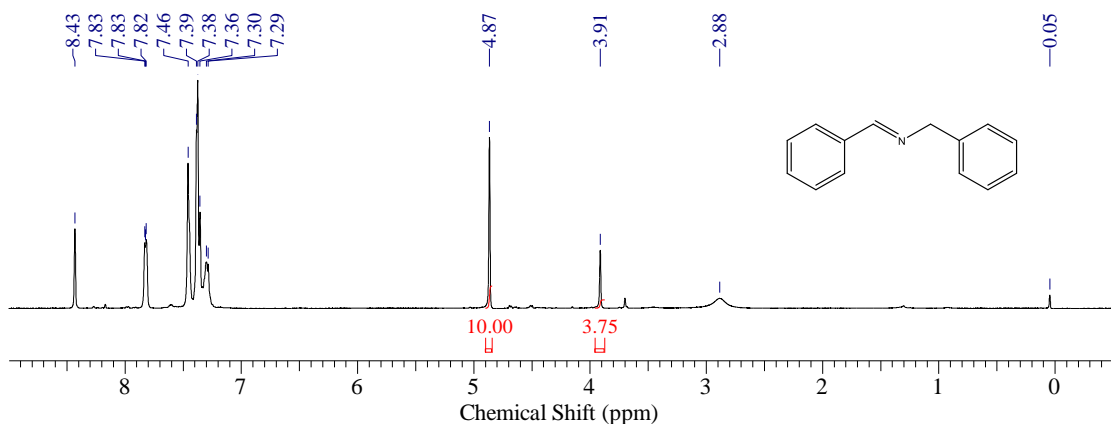


Figure S4-30. ^1H NMR(CDCl_3 , 400 MHz), Photosensitizer: DB-FL (0.5 mol%), Reaction solvent: CH_3OH , Reaction time: 7 h, Yield: 84 %.

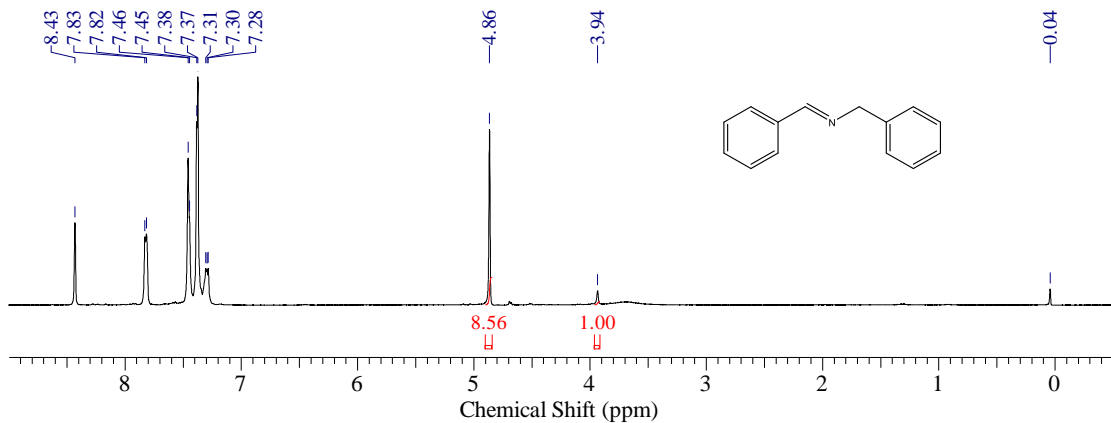


Figure S4-31. ^1H NMR(CDCl_3 , 400 MHz), Photosensitizer: DB-FL (0.5 mol%), Reaction solvent: CH_3CN , Reaction time: 7 h, Yield: 94 %.

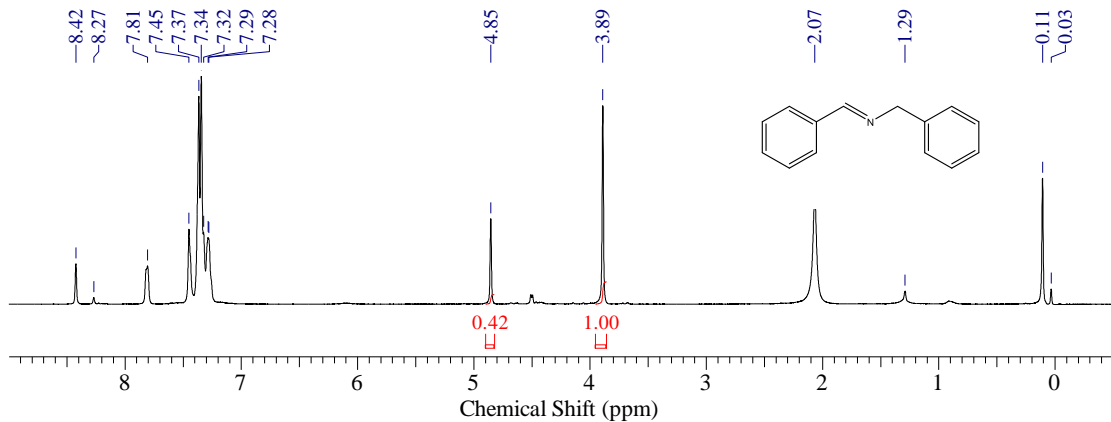


Figure S4-32. ^1H NMR(CDCl_3 , 400 MHz), Photosensitizer: DB-FL (0.5 mol%), Reaction solvent: CH_2Cl_2 , Reaction time: 7 h, Yield: 46 %.

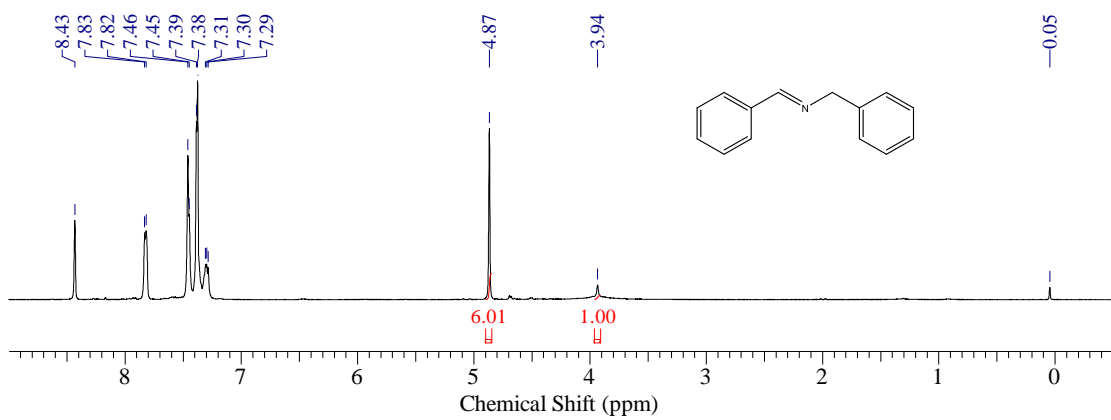


Figure S4-33. ^1H NMR(CDCl_3 , 400 MHz), Photosensitizer: DB-FL (0.5 mol%), Reaction solvent: CH_3CN : CH_3OH =9:1(v:v), Reaction time: 7 h, Yield: 92 %.

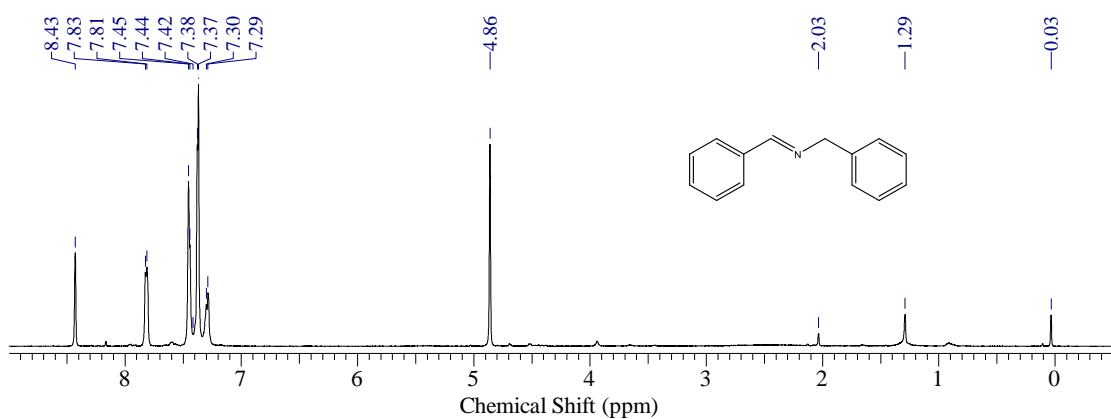
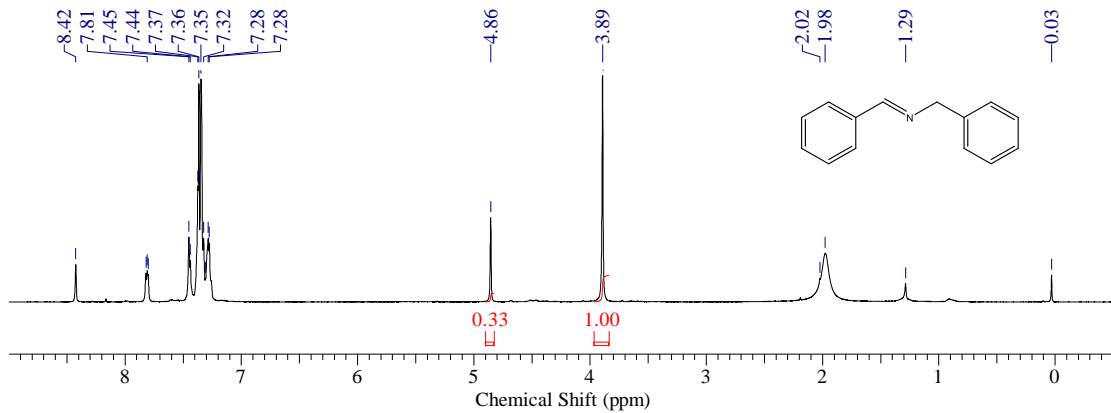


Figure S4-34. ¹H NMR(CDCl₃,400 MHz), Photosensitizer: DB-FL (0.5 mol%), Reaction solvent: CH₃CN:H₂O=9:1(v:v), Reaction time: 7 h, Yield: 100 %.



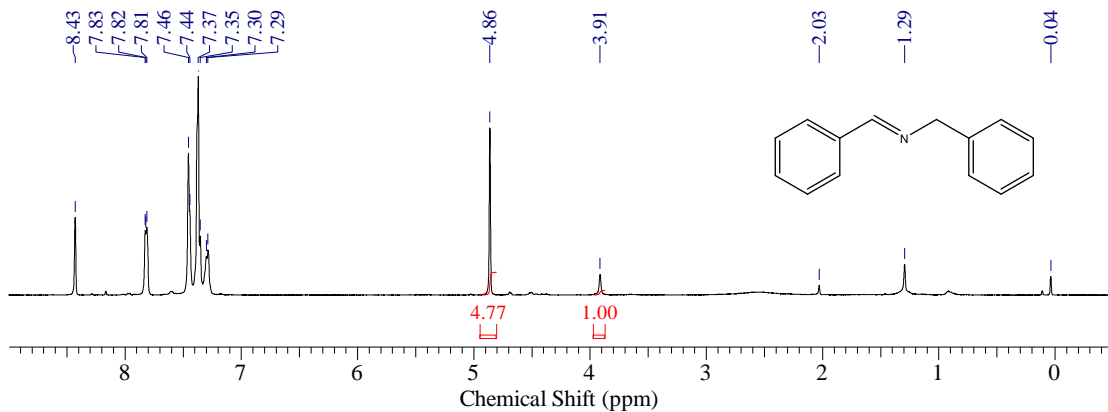


Figure S4-37. ^1H NMR(CDCl_3 , 400 MHz), Photosensitizer: DB-FL (0.5 mol%), Reaction solvent: $\text{CH}_3\text{CN}:\text{H}_2\text{O}=9:1$ (v:v), Reaction time: 5 h, Yield: 91 %.

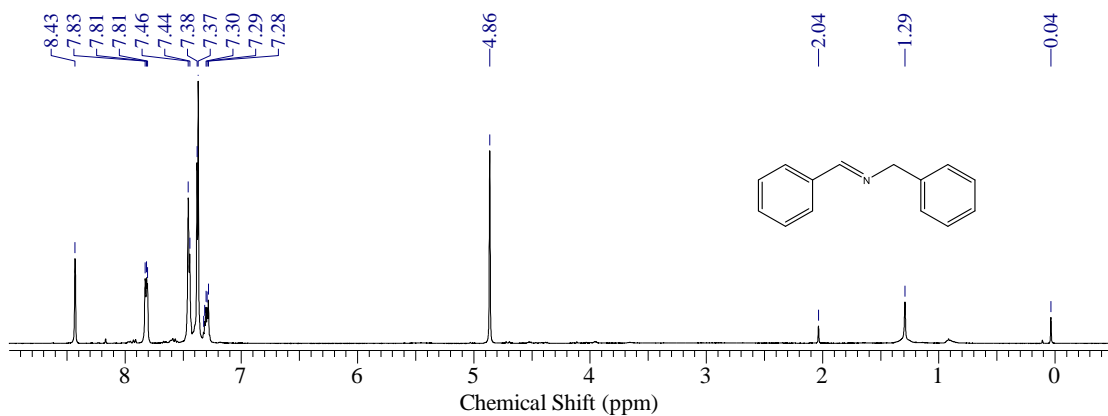


Figure S4-38. ^1H NMR(CDCl_3 , 400 MHz), Photosensitizer: DB-FL (0.5 mol%), Reaction solvent: $\text{CH}_3\text{CN}:\text{H}_2\text{O}=9:1$ (v:v), Reaction time: 9 h, Yield: 100 %.

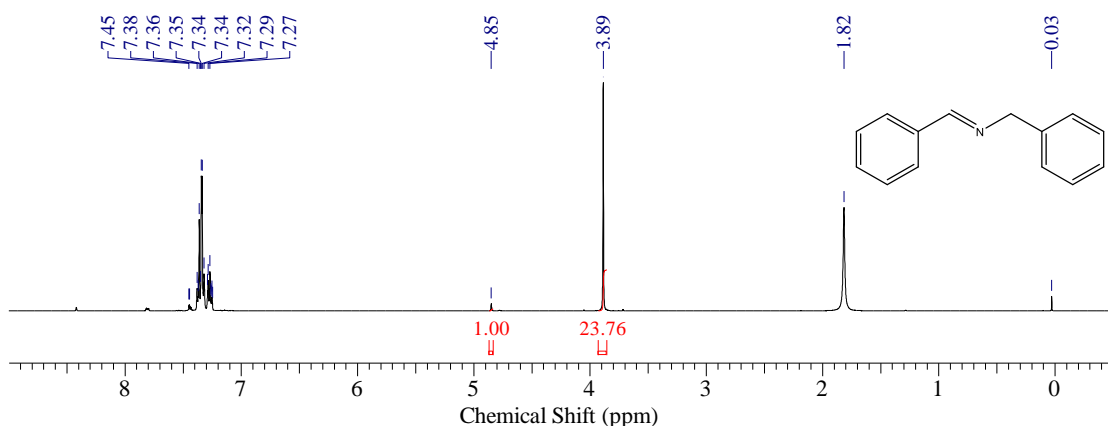


Figure S4-39. ^1H NMR(CDCl_3 , 400 MHz), Photosensitizer: Ph-FL (0.5 mol%), Reaction solvent: CH_3OH , Reaction time: 9 h, Yield: 8 %.

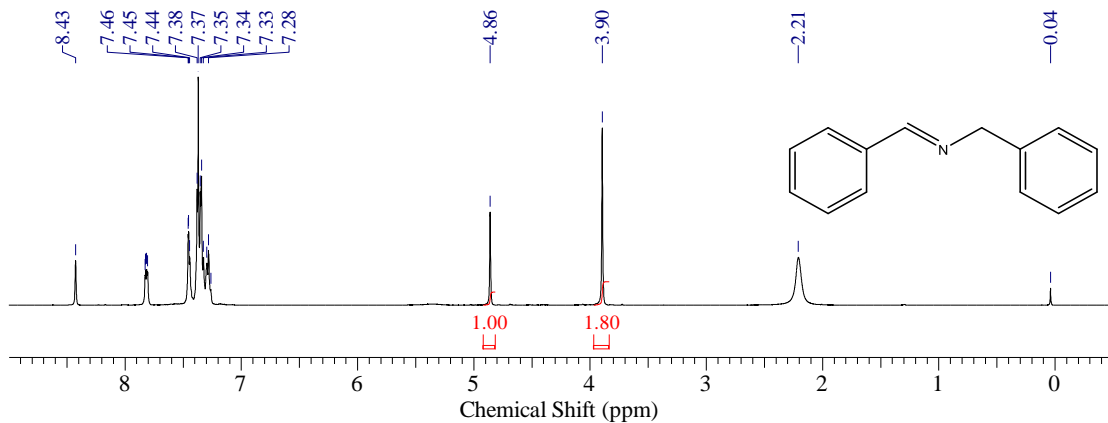


Figure S4-40. ^1H NMR(CDCl_3 , 400 MHz), Photosensitizer: Ph-FL (0.5 mol%), Reaction solvent: CH_3CN , Reaction time: 9 h, Yield: 53 %.

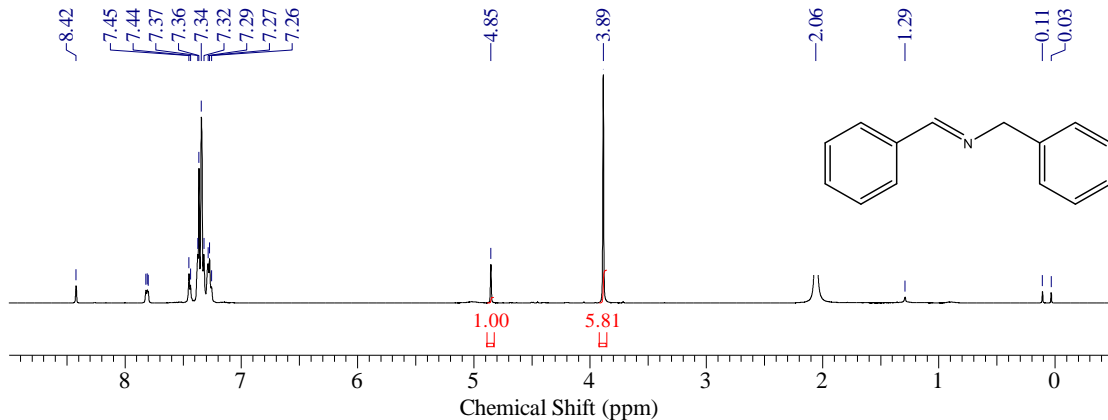


Figure S4-41. ^1H NMR(CDCl_3 , 400 MHz), Photosensitizer: Ph-FL (0.5 mol%), Reaction solvent: CH_2Cl_2 , Reaction time: 9 h, Yield: 26 %.

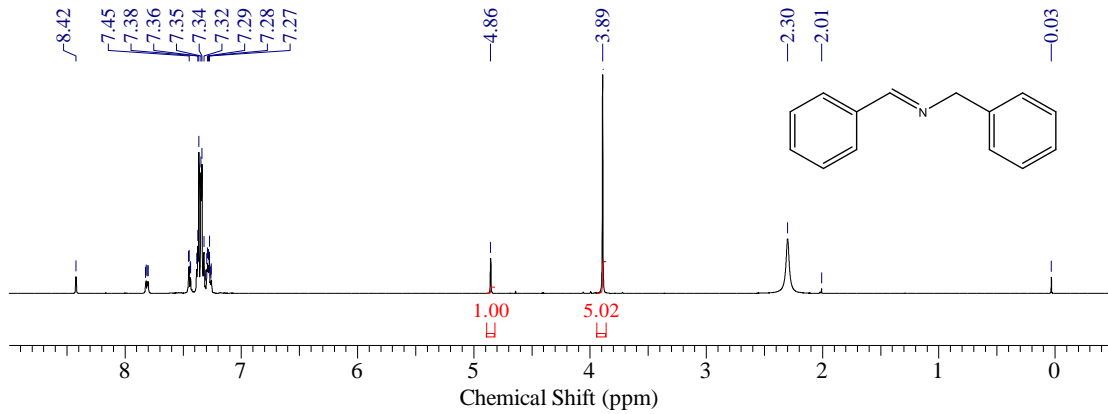


Figure S4-42. ^1H NMR(CDCl_3 , 400 MHz), Photosensitizer: Ph-FL (0.5 mol%), Reaction solvent: $\text{CH}_3\text{CN}:\text{CH}_3\text{OH} = 9:1$ (v:v), Reaction time: 9 h, Yield: 28 %.

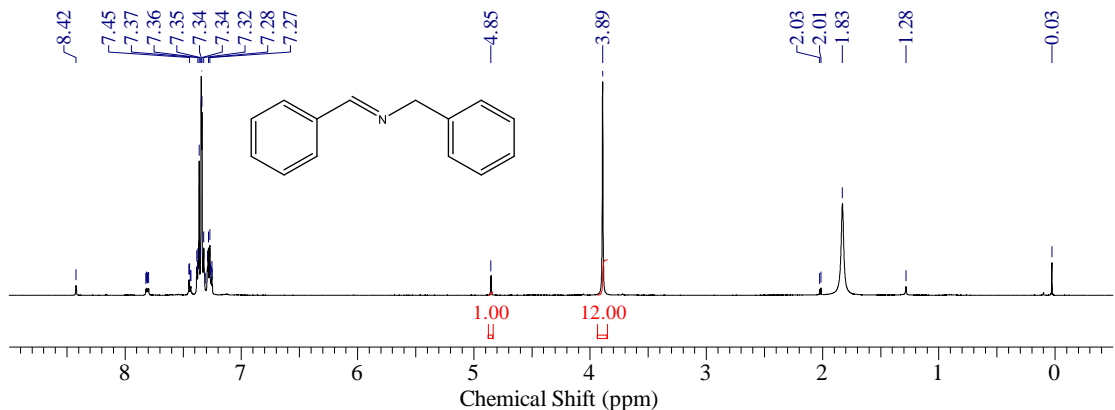


Figure S4-43. ^1H NMR(CDCl_3 , 400 MHz), Photosensitizer: Ph-FL (0.5 mol%), Reaction solvent: $\text{CH}_3\text{CN}:\text{H}_2\text{O} = 9:1$ (v:v), Reaction time: 9 h, Yield: 14 %.

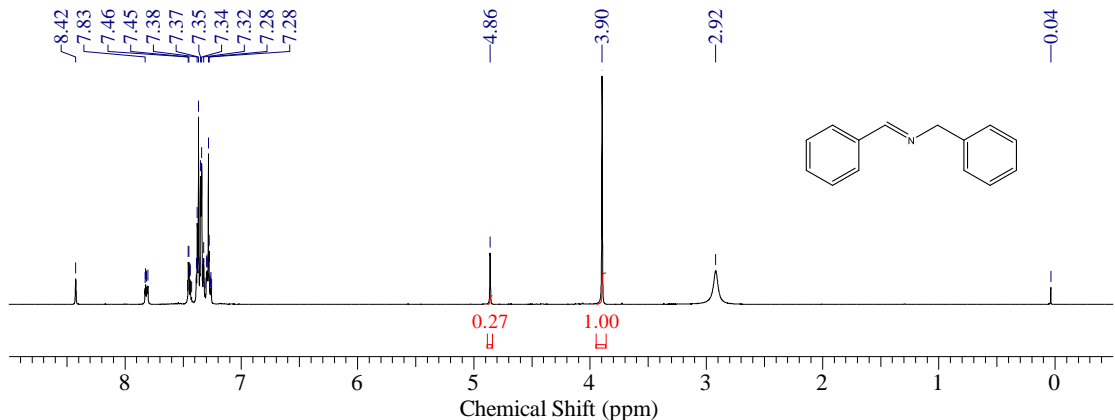


Figure S4-44. ^1H NMR(CDCl_3 , 400 MHz), Photosensitizer: Ph-FL (0.5 mol%), Reaction solvent: CH_3CN , Reaction time: 3 h, Yield: 35 %.

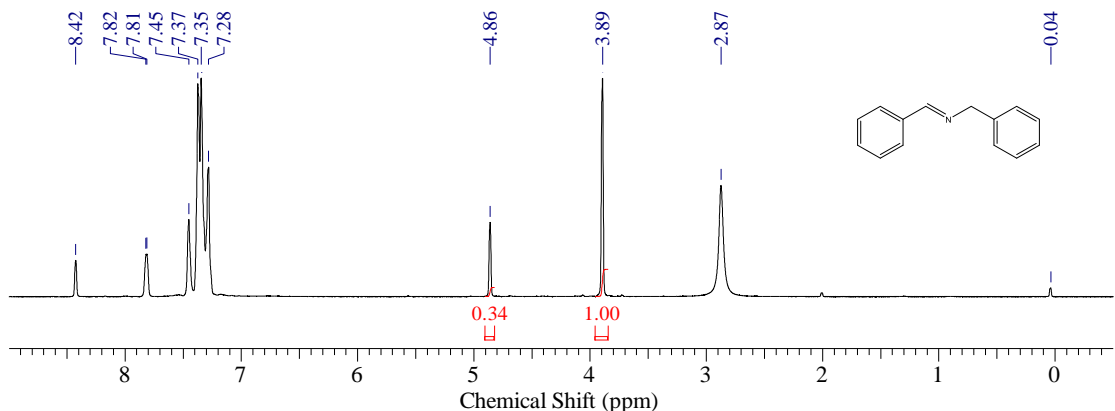


Figure S4-45. ^1H NMR(CDCl_3 , 400 MHz), Photosensitizer: Ph-FL (0.5 mol%), Reaction solvent: CH_3CN , Reaction time: 5 h, Yield: 40 %.

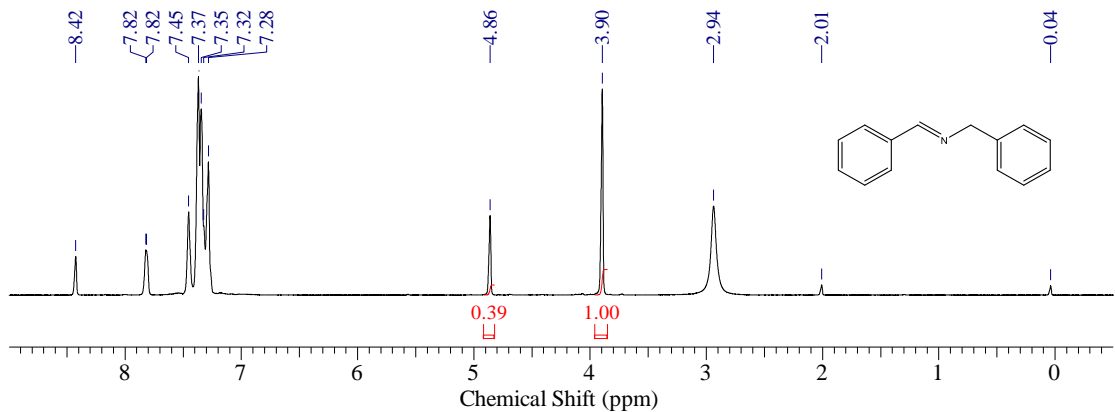


Figure S4-46. ^1H NMR(CDCl_3 , 400 MHz), Photosensitizer: Ph-FL (0.5 mol%), Reaction solvent: CH_3CN , Reaction time: 7 h, Yield: 44 %.

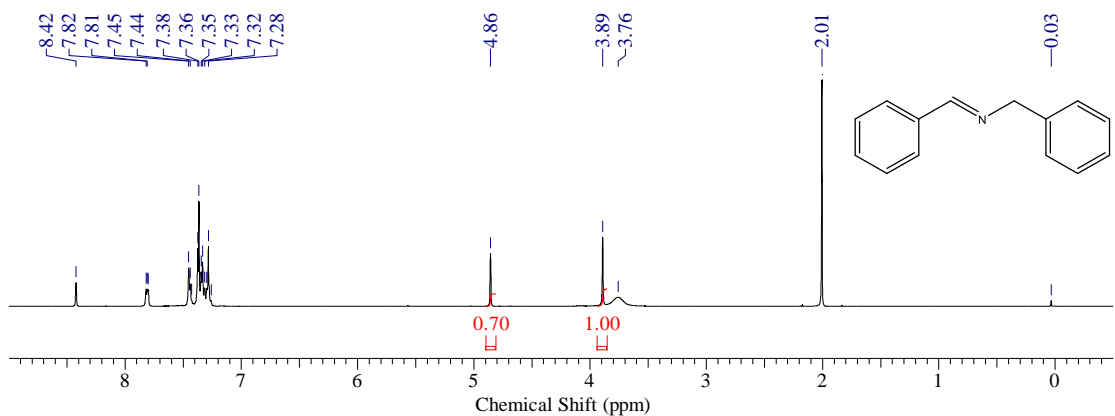


Figure S4-47. ^1H NMR(CDCl_3 , 400 MHz), Photosensitizer: Ph-FL (0.5 mol%), Reaction solvent: CH_3CN , Reaction time: 11 h, Yield: 58 %.

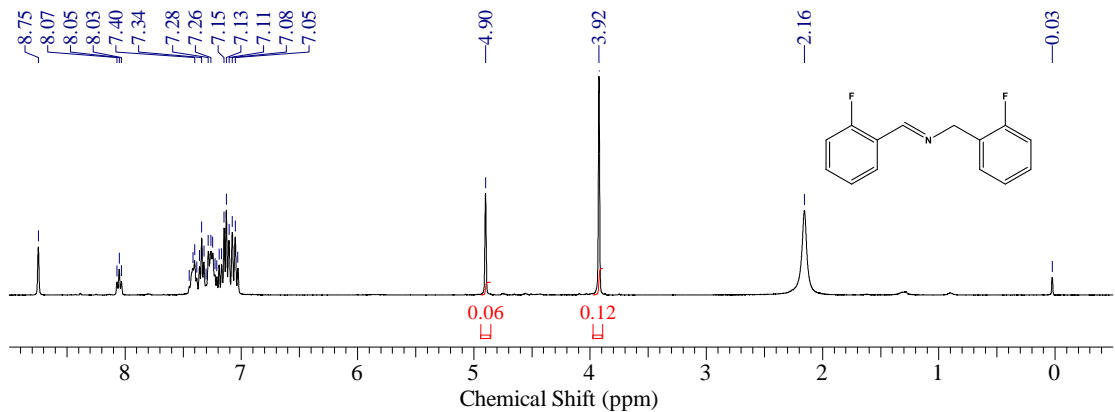


Figure S4-48. ^1H NMR(CDCl_3 , 400 MHz), Photosensitizer: FL(0.5 mol%), Reaction solvent: CH_3CN , Reaction time: 9 h, Yield: 50 %.

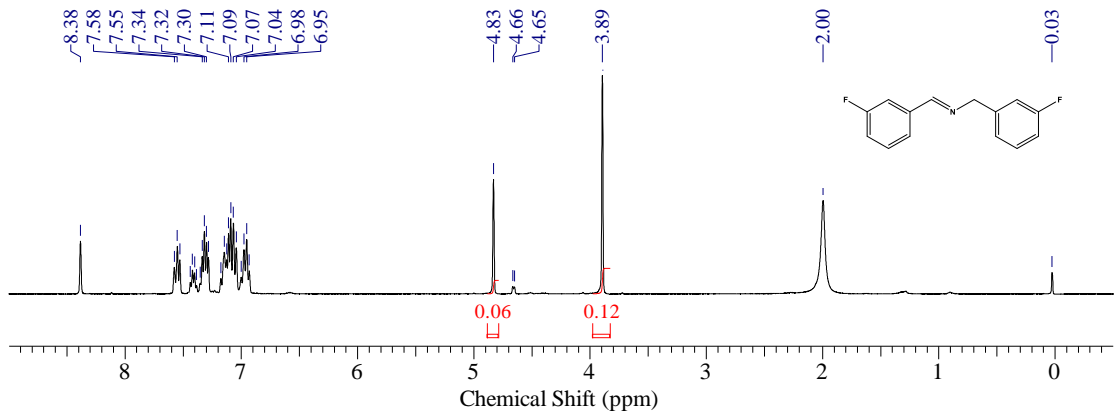


Figure S4-49. ^1H NMR(CDCl_3 , 400 MHz), Photosensitizer: FL(0.5 mol%), Reaction solvent: CH_3CN , Reaction time: 9 h, Yield: 50 %.

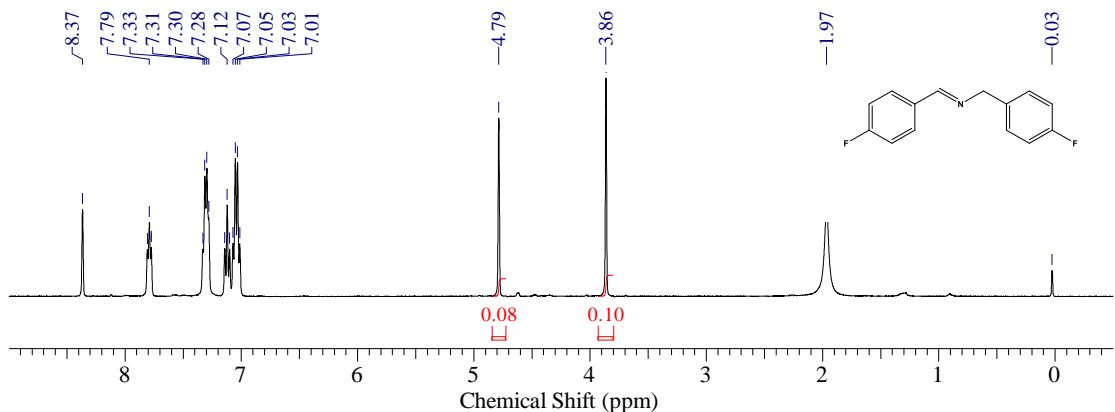


Figure S4-50. ^1H NMR(CDCl_3 , 400 MHz), Photosensitizer: FL(0.5 mol%), Reaction solvent: CH_3CN , Reaction time: 9 h, Yield: 62 %.

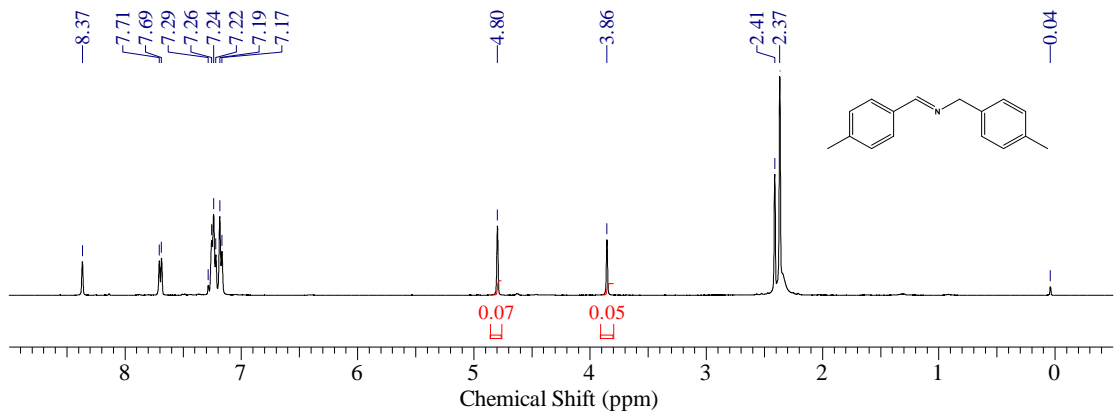


Figure S4-51. ^1H NMR(CDCl_3 , 400 MHz), Photosensitizer: FL(0.5 mol%), Reaction solvent: CH_3CN , Reaction time: 9 h, Yield: 74 %.

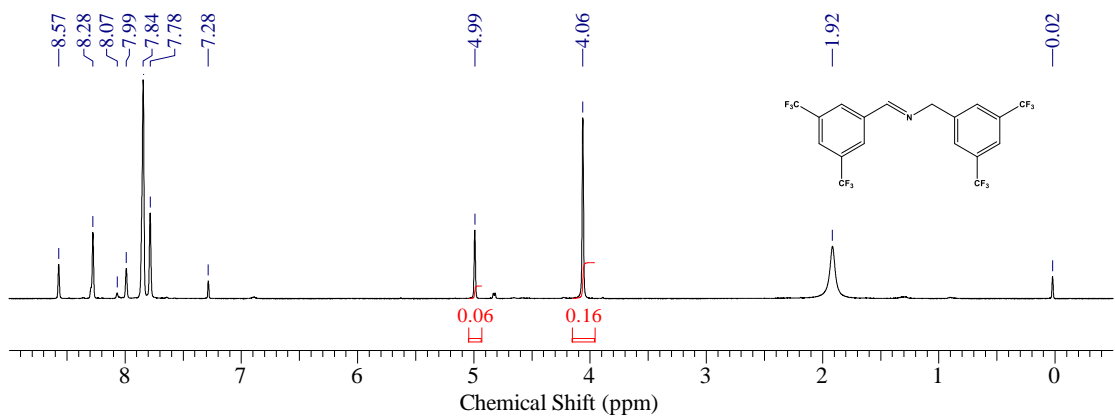


Figure S4-52. ^1H NMR(CDCl_3 , 400 MHz), Photosensitizer: FL(0.5 mol%), Reaction solvent: CH_3CN , Reaction time: 9 h, Yield: 43 %.

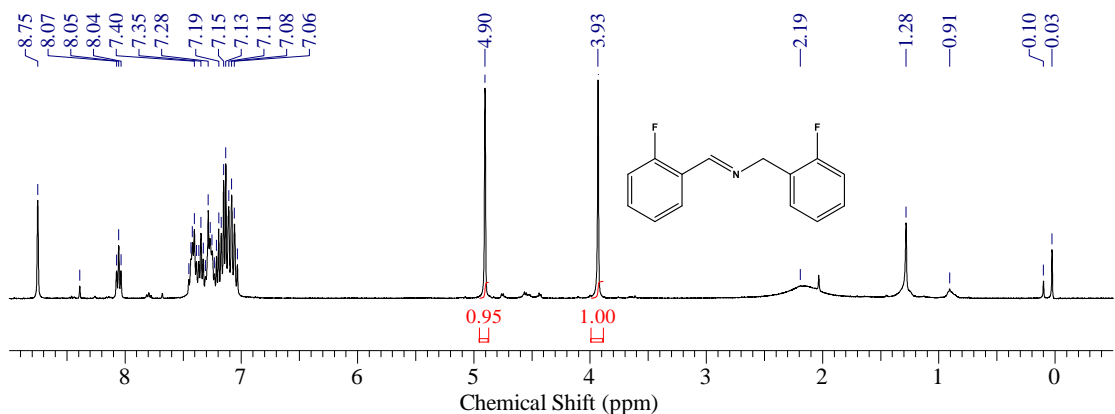


Figure S4-53. ^1H NMR(CDCl_3 , 400 MHz), Photosensitizer: MB-FL (0.5 mol%), Reaction solvent: $\text{CH}_3\text{CN}:\text{H}_2\text{O}=9:1(\text{v}: \text{v})$, Reaction time: 9 h, Yield: 66 %.

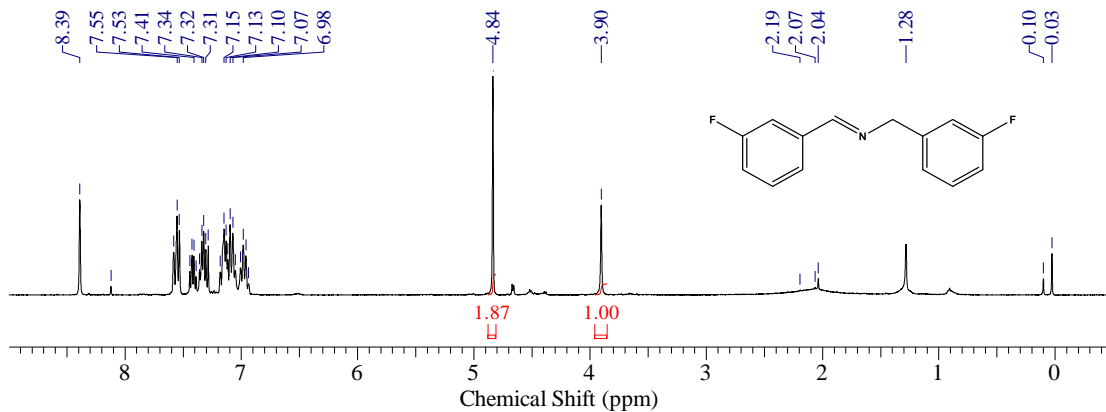


Figure S4-54. ^1H NMR(CDCl_3 , 400 MHz), Photosensitizer: MB-FL (0.5 mol%), Reaction solvent: $\text{CH}_3\text{CN}:\text{H}_2\text{O} = 9:1$ (v:v), Reaction time: 9 h, Yield: 79 %.

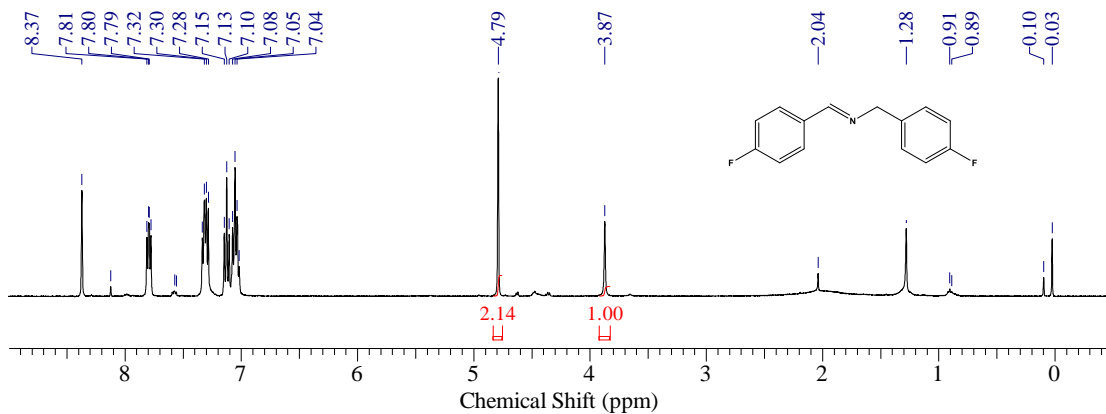


Figure S4-55. ^1H NMR(CDCl_3 , 400 MHz), Photosensitizer: MB-FL (0.5 mol%), Reaction solvent: $\text{CH}_3\text{CN}:\text{H}_2\text{O} = 9:1$ (v:v), Reaction time: 9 h, Yield: 81 %.

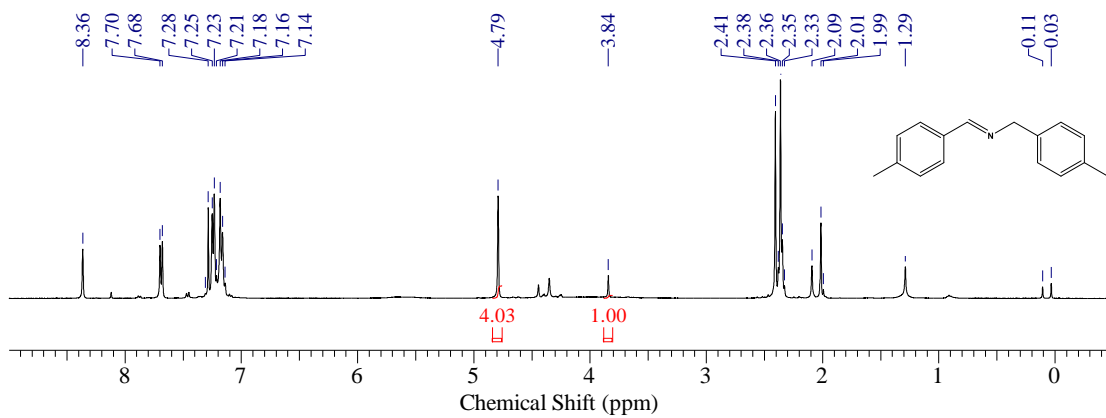


Figure S4-56. ^1H NMR(CDCl_3 , 400 MHz), Photosensitizer: MB-FL (0.5 mol%), Reaction solvent: $\text{CH}_3\text{CN}:\text{H}_2\text{O} = 9:1$ (v:v), Reaction time: 9 h, Yield: 89 %.

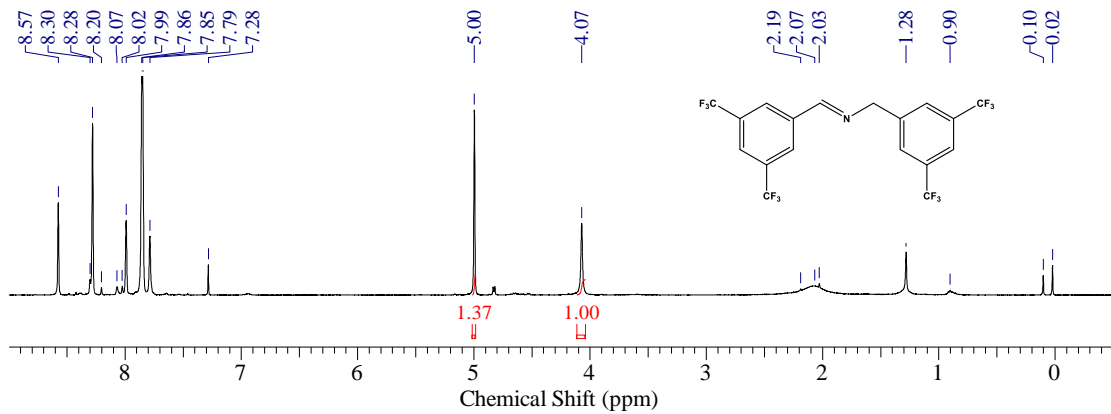


Figure S4-57. ^1H NMR(CDCl_3 , 400 MHz), Photosensitizer: MB-FL (0.5 mol%), Reaction solvent: $\text{CH}_3\text{CN}:\text{H}_2\text{O}=9:1$ (v:v), Reaction time: 9 h, Yield: 73 %.

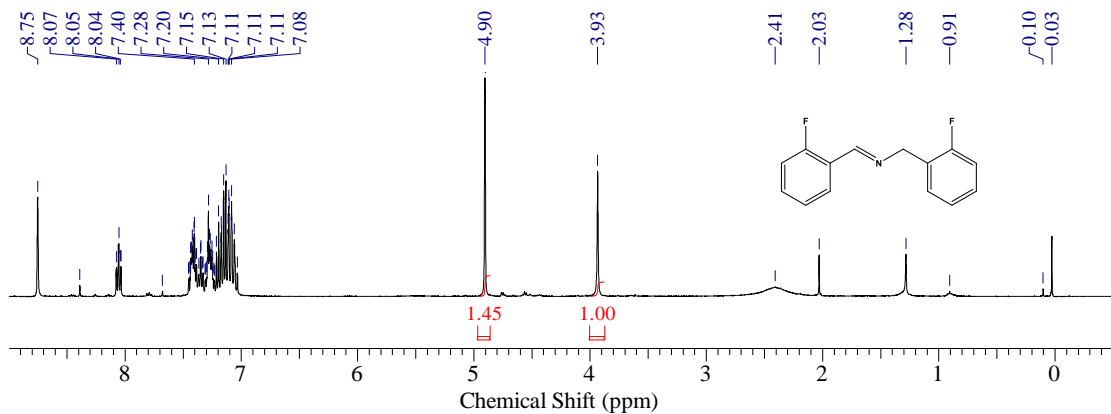


Figure S4-58.¹H NMR(CDCl₃,400 MHz), Photosensitizer: DB-FL (0.5 mol%), Reaction solvent: CH₃CN:H₂O=9:1(v:v), Reaction time: 5 h, Yield: 74 %.

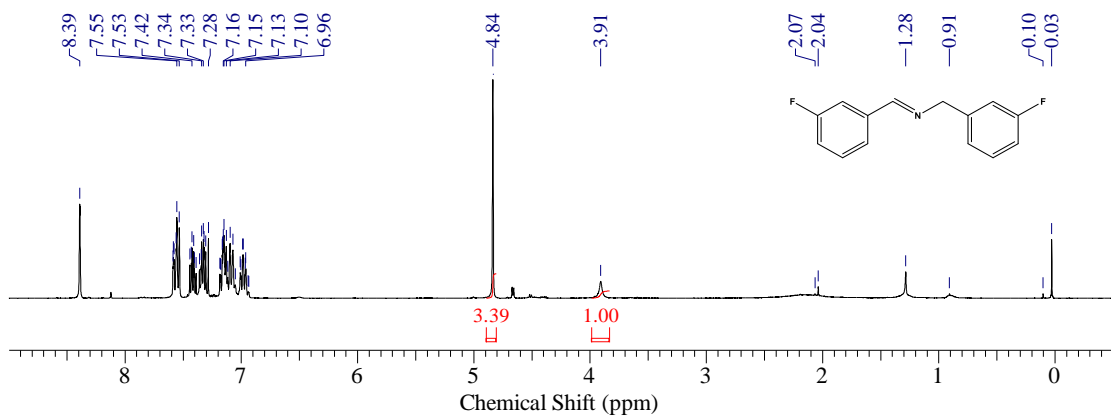


Figure S4-59. ^1H NMR(CDCl_3 , 400 MHz), Photosensitizer: DB-FL (0.5 mol%), Reaction solvent: $\text{CH}_3\text{CN}:\text{H}_2\text{O}=9:1$ (v:v), Reaction time: 5 h, Yield: 87 %.

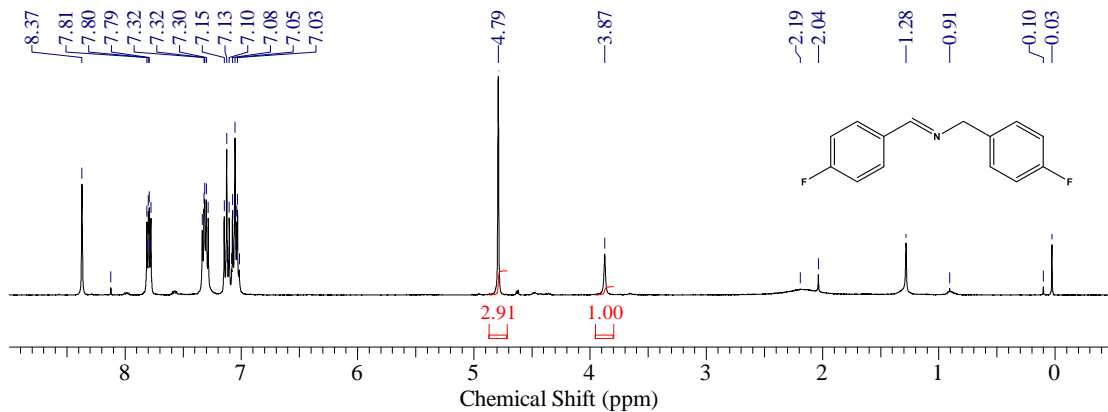


Figure S4-60. ^1H NMR (CDCl_3 , 400 MHz), Photosensitizer:DB-FL (0.5 mol%), Reaction solvent: $\text{CH}_3\text{CN}:\text{H}_2\text{O} = 9:1$ (v:v), Reaction time: 5 h, Yield: 85 %.

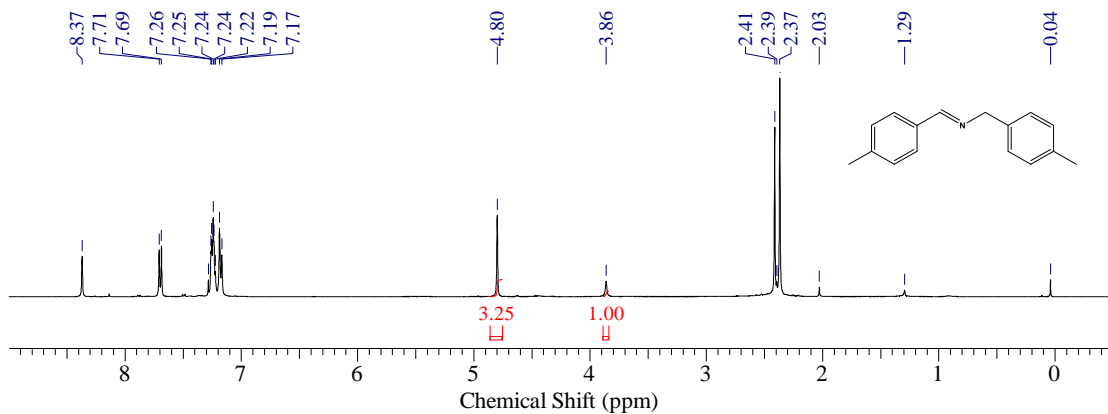


Figure S4-61. ^1H NMR(CDCl_3 ,400 MHz), Photosensitizer: DB-FL (0.5 mol%), Reaction solvent: $\text{CH}_3\text{CN}:\text{H}_2\text{O} = 9:1$ (v:v), Reaction time: 5 h, Yield: 87 %.

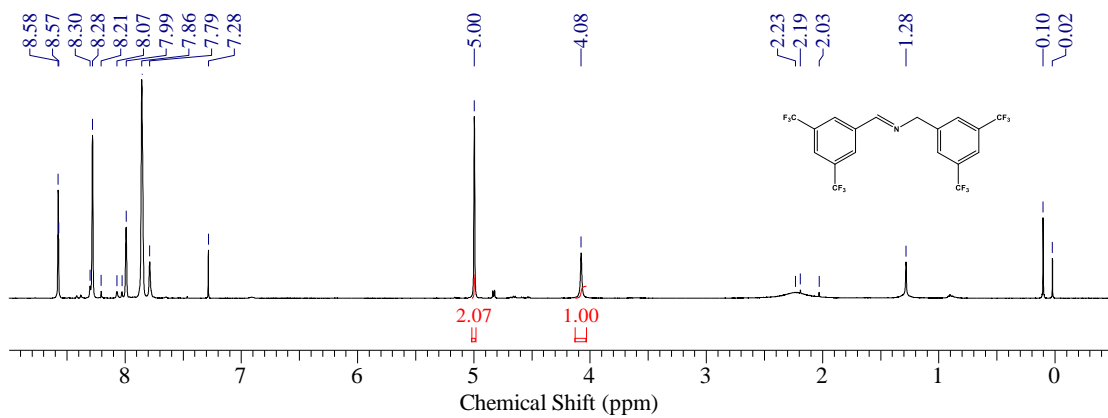


Figure S4-62. ^1H NMR(CDCl_3 ,400 MHz), Photosensitizer: DB-FL (0.5 mol%), Reaction solvent: $\text{CH}_3\text{CN}:\text{H}_2\text{O} = 9:1$ (v:v), Reaction time:5 h, Yield: 81 %.

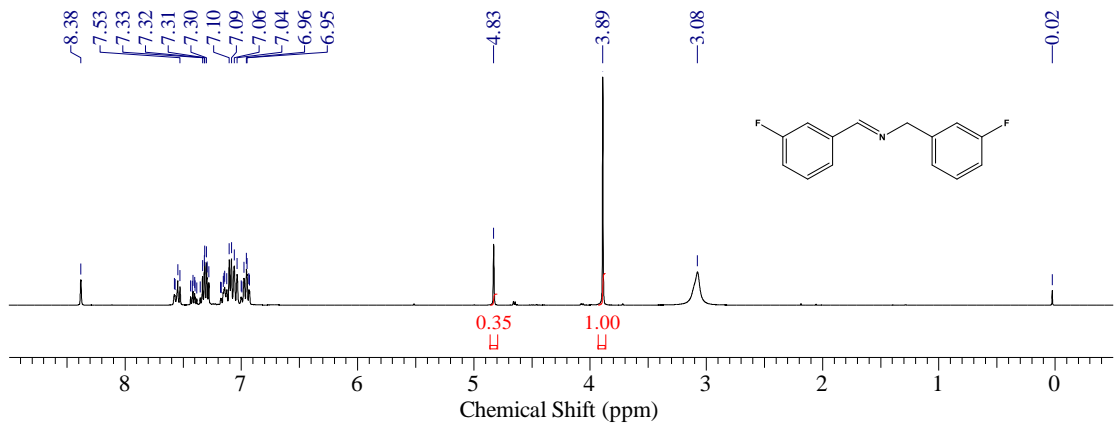


Figure S4-63. ^1H NMR(CDCl_3 ,400 MHz), Photosensitizer: Ph-FL (0.5 mol%), Reaction solvent: CH_3CN , Reaction time: 9 h, Yield: 41 %.

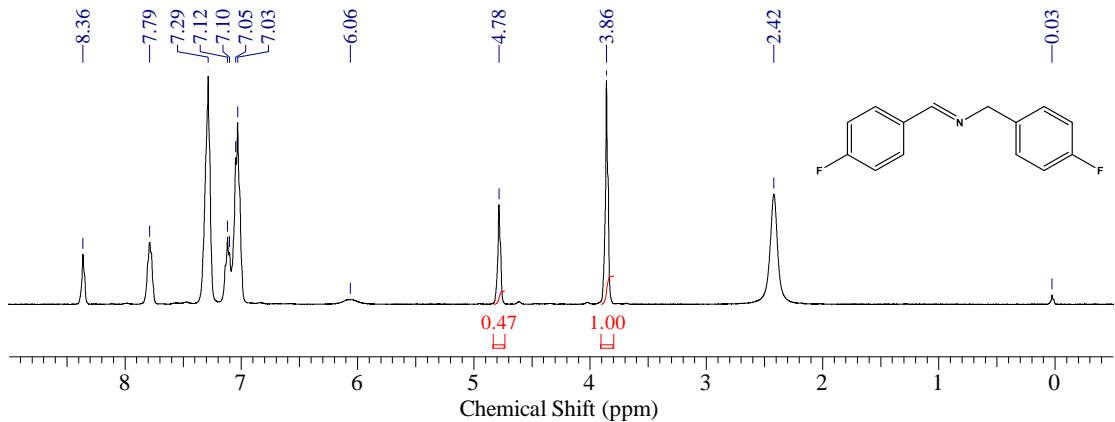


Figure S4-64. ^1H NMR (CDCl_3 ,400 MHz), Photosensitizer:Ph-FL (0.5 mol%), Reaction solvent: CH_3CN , Reaction time: 9 h, Yield:48 %.

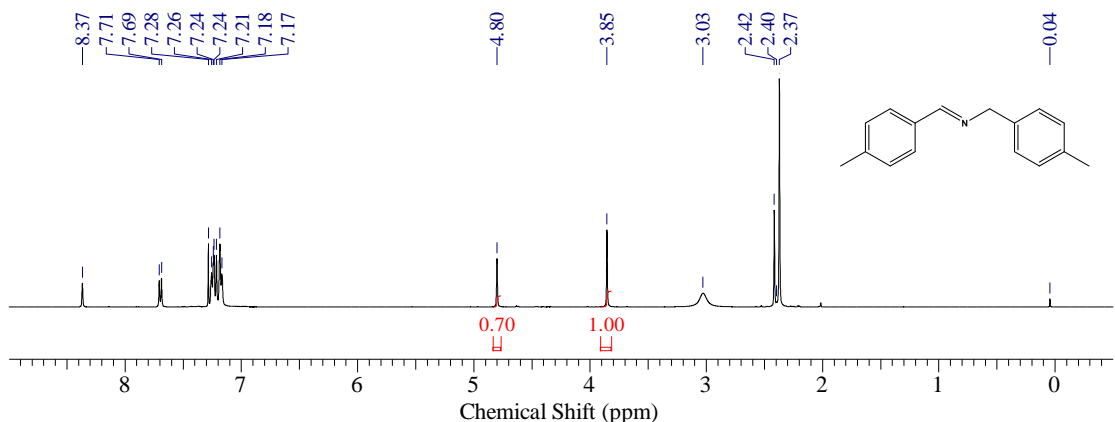


Figure S4-65. ^1H NMR (CDCl_3 ,400 MHz), Photosensitizer: Ph-FL (0.5 mol%), Reaction solvent: CH_3CN , Reaction time: 9 h, Yield: 60 %.

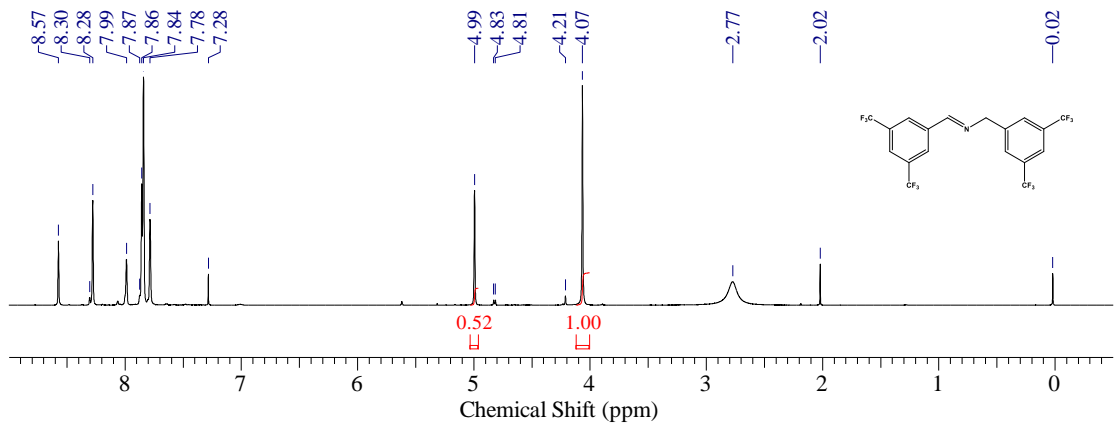


Figure S4-66. ^1H NMR (CDCl_3 , 400 MHz), Photosensitizer: Ph-FL (0.5 mol%), Reaction solvent: CH_3CN , Reaction time: 9 h, Yield: 60 %.

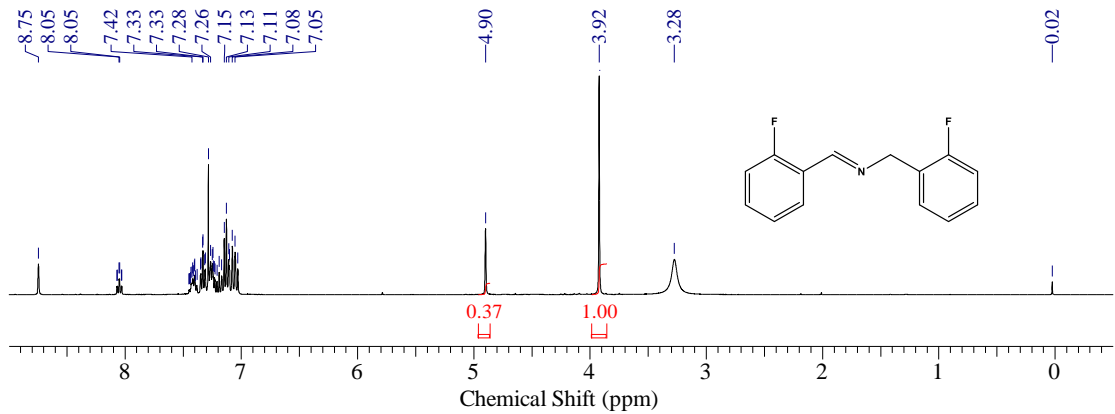


Figure S4-67. ^1H NMR(CDCl_3 , 400 MHz), Photosensitizer: Ph-FL (0.5 mol%), Reaction solvent: CH_3CN , Reaction time: 9 h, Yield: 43 %.

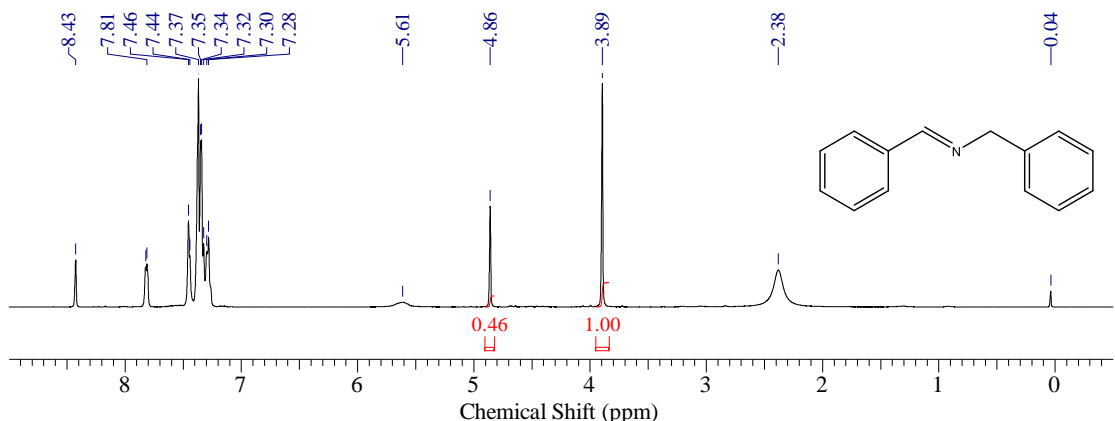


Figure S4-68. ^1H NMR (CDCl_3 , 400 MHz), Photosensitizer: FL (0.5 mol%), Trapping agent: DABCO(0.5 mol%), Reaction solvent: CH_3CN , Reaction time: 9 h, Yield: 48 %.

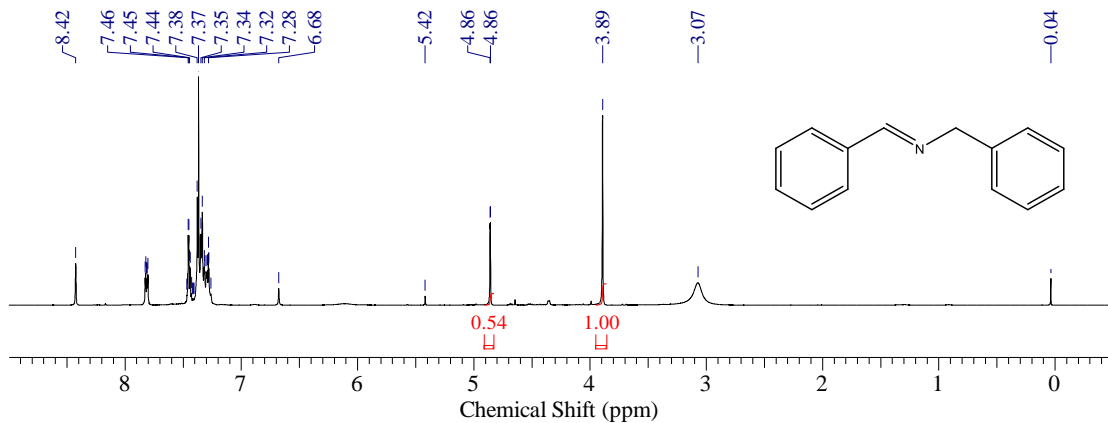


Figure S4-69. ^1H NMR(CDCl_3 , 400 MHz), Photosensitizer: FL (0.5 mol%), Trapping agent: BQ(0.5 mol%), Reaction solvent: CH_3CN , Reaction time: 9 h, Yield: 52 %.

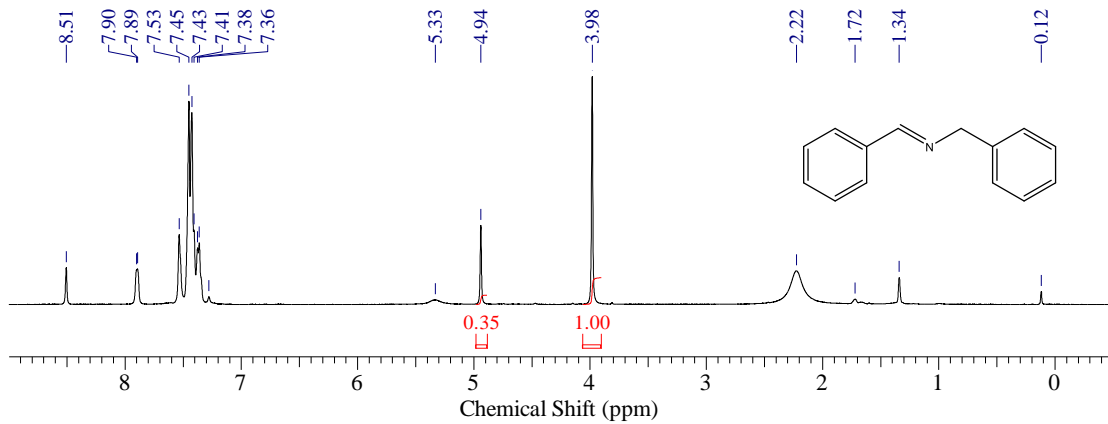


Figure S4-70. ^1H NMR(CDCl_3 , 400 MHz), Photosensitizer: FL (0.5 mol%), Trapping agent: TEMPO(15 mol%), Reaction solvent: CH_3CN , Reaction time: 9 h, Yield: 41 %.

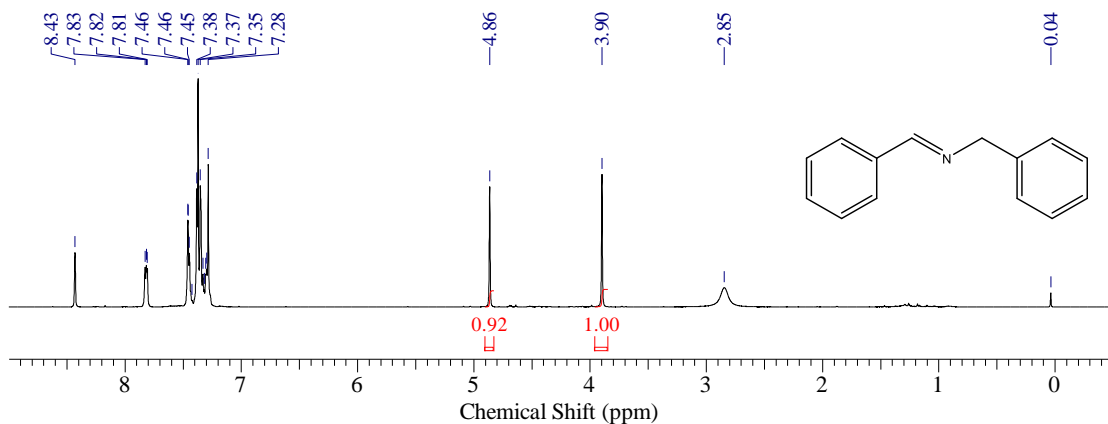


Figure S4-71. ^1H NMR(CDCl_3 , 400 MHz), Photosensitizer: FL (0.5 mol%), Trapping agent: BHT(15 mol%), Reaction solvent: CH_3CN , Reaction time: 9 h, Yield: 65 %.

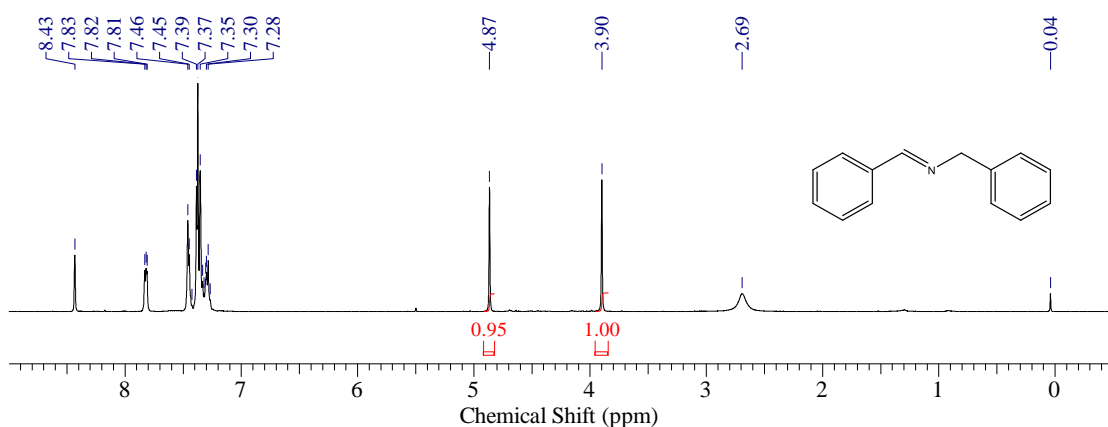


Figure S4-72. ^1H NMR(CDCl_3 , 400 MHz), Photosensitizer: FL (0.5 mol%), Trapping agent: DDUN(15 mol%), Reaction solvent: CH_3CN , Reaction time: 9 h, Yield: 66 %.

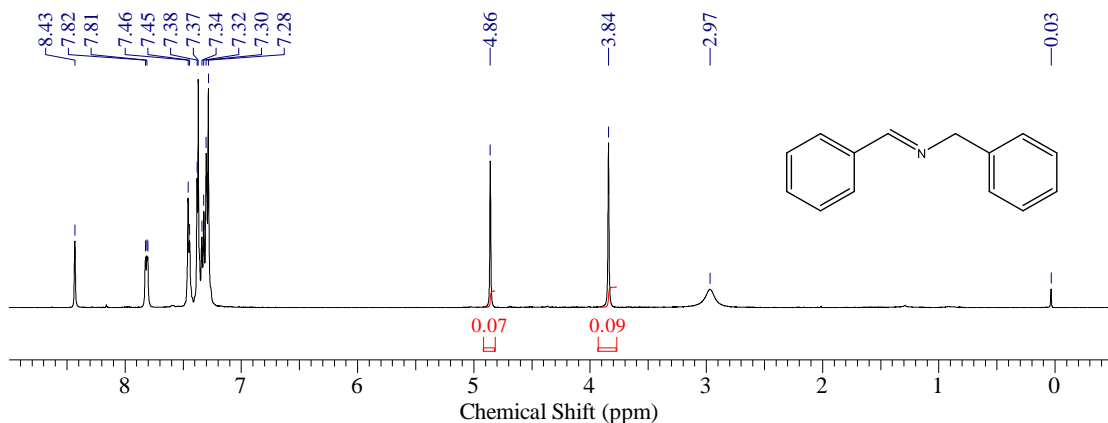


Figure S4-73. ^1H NMR (CDCl_3 , 400 MHz), Photosensitizer: FL (0.5 mol%), Trapping agent: AgNO_3 (0.5 mol%), Reaction solvent: CH_3CN , Reaction time: 9 h, Yield: 61 %.

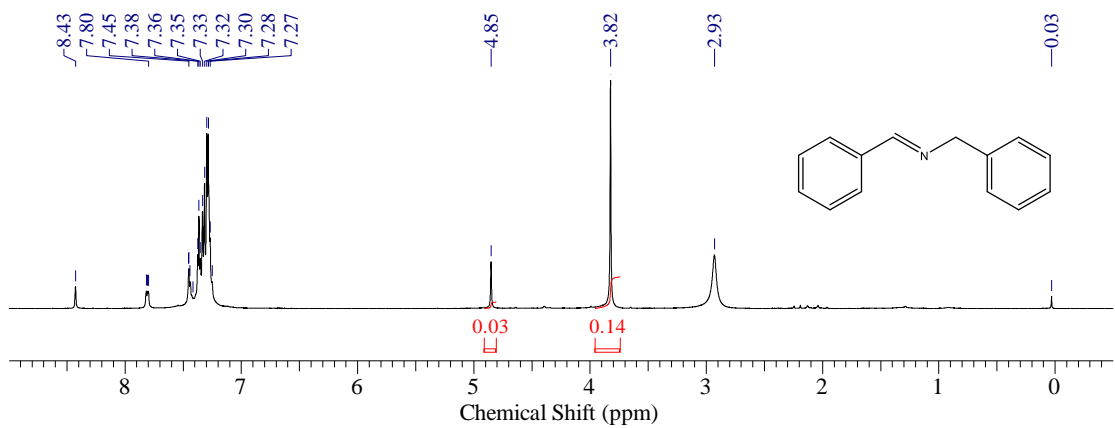


Figure S4-74. ^1H NMR (CDCl_3 , 400 MHz), Photosensitizer: FL (0.5 mol%), Trapping agent: AgNO_3 (15 mol%), Reaction solvent: CH_3CN , Reaction time: 9 h, Yield: 30 %.

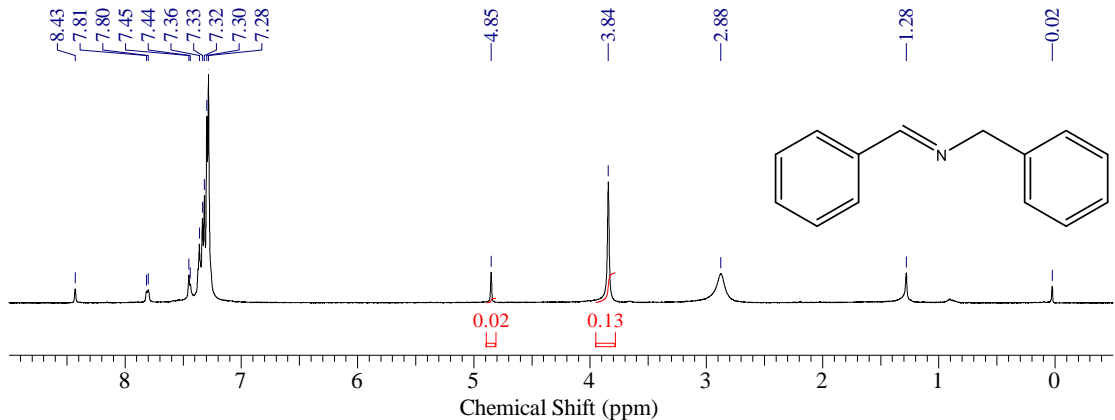


Figure S4-75. ^1H NMR (CDCl_3 , 400 MHz), Photosensitizer: FL (0.5 mol%), Trapping agent: AgNO_3 (25 mol%), Reaction solvent: CH_3CN , Reaction time: 9 h, Yield: 24 %.

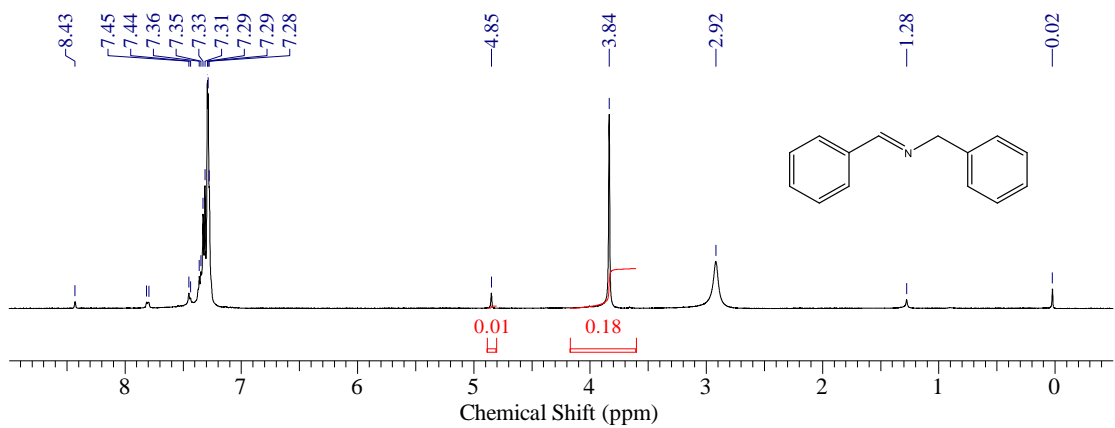


Figure S4-76. ^1H NMR(CDCl_3 , 400 MHz), Photosensitizer: Ph-FL (0.5 mol%), Trapping agent: AgNO_3 (25 mol%), Reaction solvent: CH_3CN , Reaction time: 9 h, Yield: 10 %.

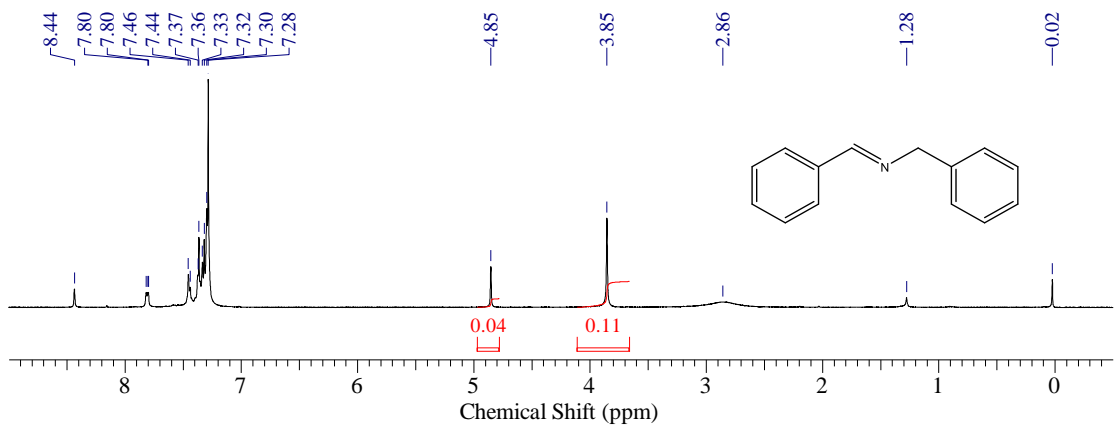


Figure S4-77. ^1H NMR(CDCl_3 , 400 MHz), Photosensitizer: MB-FL (0.5 mol%), Trapping agent: AgNO_3 (25 mol%), Reaction solvent: CH_3CN , Reaction time: 9 h, Yield: 42 %.

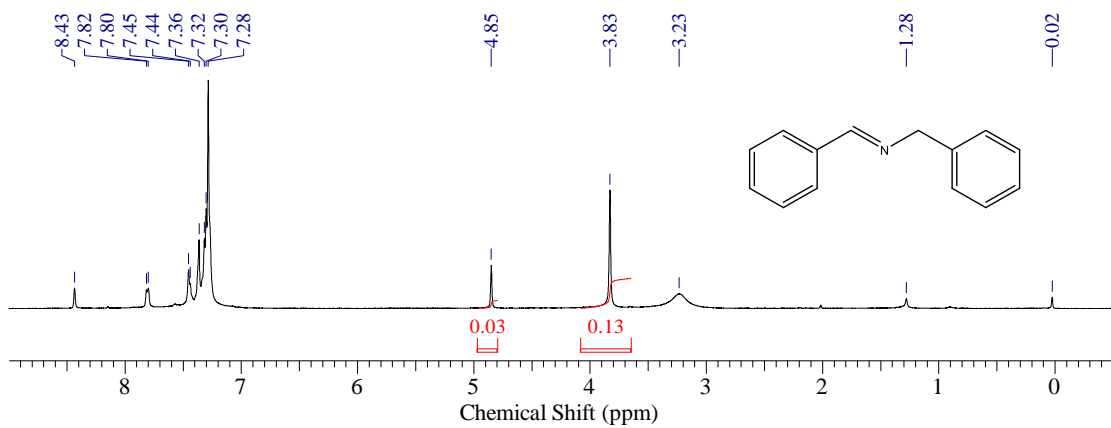


Figure S4-78. ^1H NMR(CDCl_3 , 400 MHz), Photosensitizer: DB-FL (0.5 mol%), Trapping agent: AgNO_3 (25 mol%), Reaction solvent: CH_3CN : H_2O =9:1(v:v), Reaction time: 5 h, Yield: 32 %.

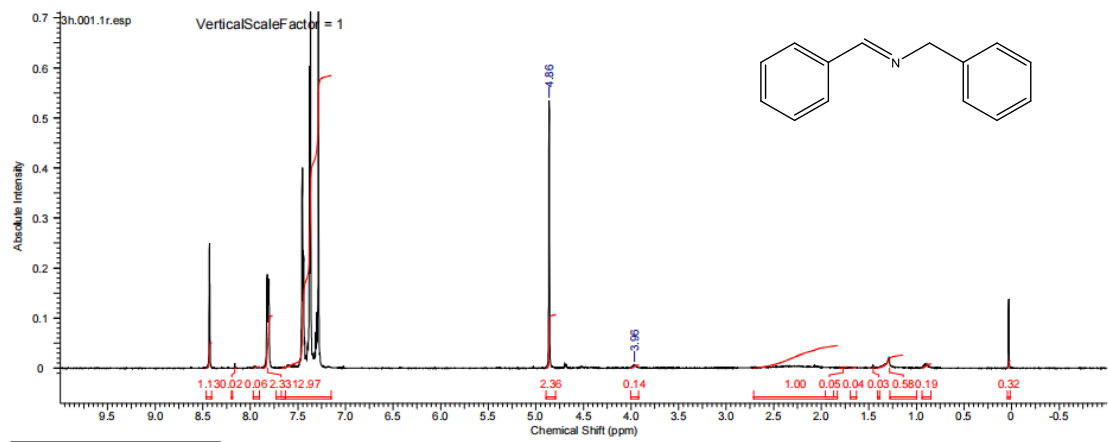


Figure S4-79. ^1H NMR(CDCl_3 , 400 MHz), Photosensitizer: DB-FL (0.5 mol%), Reaction solvent: CD_3CN : H_2O =9:1(v:v), Reaction time: 3 h, Yield: 94.4 %.

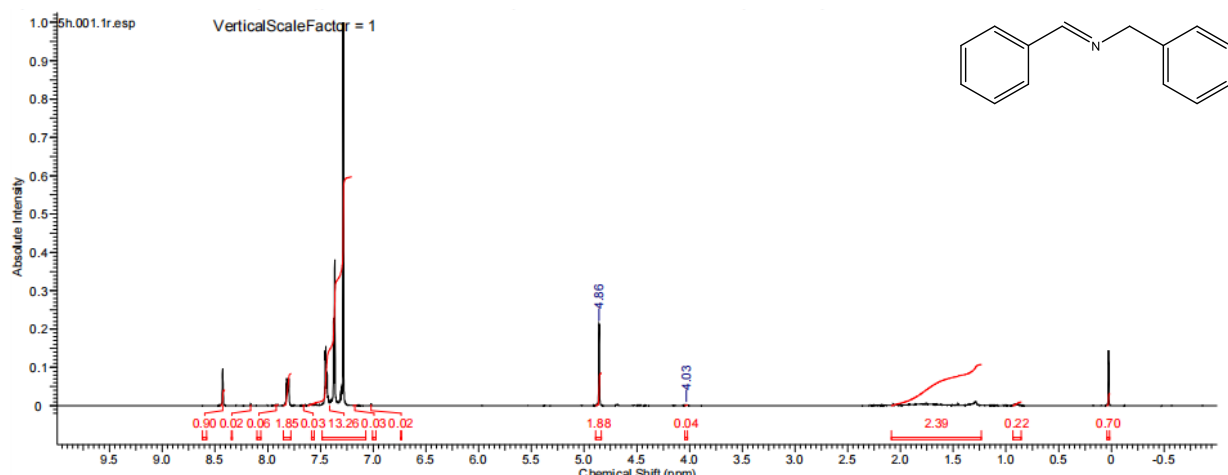


Figure S4-80. ^1H NMR(CDCl_3 , 400 MHz), Photosensitizer: DB-FL (0.5 mol%), Reaction solvent: $\text{CD}_3\text{CN} : \text{H}_2\text{O} = 9:1$ (v:v), Reaction time: 5 h, Yield: 97.9 %.

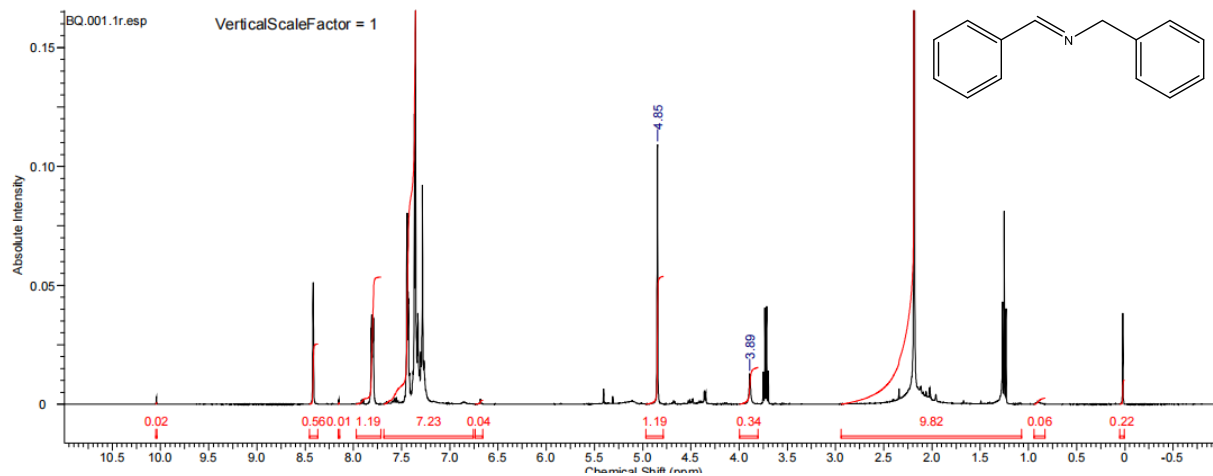


Figure S4-81. ^1H NMR(CDCl_3 , 400 MHz), Photosensitizer: DB-FL (0.5 mol%), Trapping agent: BQ, Reaction solvent: $\text{CH}_3\text{CN} : \text{H}_2\text{O} = 9:1$ (v:v), Reaction time: 5 h, Yield: 77.7 %.

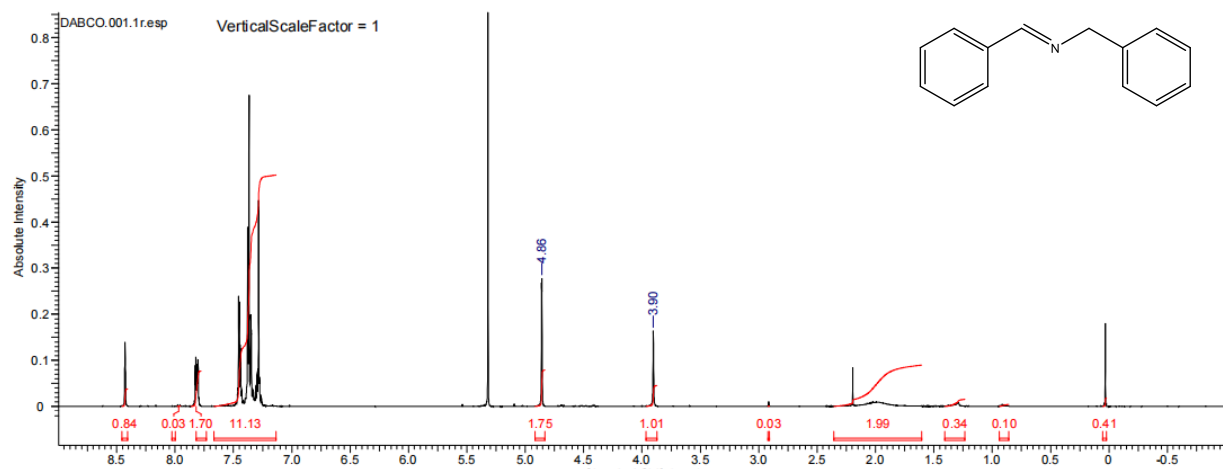


Figure S4-82. ¹H NMR(CDCl_3 ,400 MHz), Photosensitizer: DB-FL (0.5 mol%), Trapping agent:DABCO, Reaction solvent: CH_3CN : $\text{H}_2\text{O}=9:1(\text{v}: \text{v})$, Reaction time:5 h, Yield:63.4 %.

5. DFT/TD-DFT Results

Theoretical Methods

The electronic structure and photophysical properties of these sensitizers were investigated with Density Functional Theory (DFT) and Time-dependent (TD)-DFT based calculations. The alkyl groups in chromophores were simplified to $-\text{CH}_3$. S_0 structures of sensitizers were fully optimized with 6-311G(d) basis sets¹⁻³ and B3LYP functional.^{4, 5} The impact of potential interactions with solvents to electronic structure of sensitizers were treated with Polarizable Continuum Model (PCM).⁶⁻⁸ Structures of sensitizers at S_1 and T_n were obtained by relaxation with TD-DFT calculations based on the S_0 structures. These calculations were performed with Gaussian 16.⁹ The T_n to S_0 transition dipole moments were evaluated with quadratic response function¹⁰⁻¹² and the spin-orbit coupling constants were calculated with Dalton with effective single electron approximation in linear response theory.¹³⁻¹⁵ With the electronic structure of sensitizers at S_0 and excited states, photophysical properties of these FLPSs were investigated within the Thermal Vibration Correlation Function (TVCF) formalism as implemented in MOMAP.¹⁶⁻²⁰

Table S5-1. Electronic transitions involved in the excitation of FL.

FL	Energy	f	Composition	CI	Character
S ₀ →S ₁	3.0227 eV/410.18 nm	0.2152	59 → 60	0.69596	$\pi \rightarrow \pi^*, n \rightarrow \pi^*$
S ₀ →S ₂	3.3227 eV/373.14 nm	0.0008	56 → 60 57 → 60	0.50597 0.48175	n→ π^* n→ π^*
S ₀ →S ₃	3.4569 eV/358.66 nm	0.0001	54 → 60 56 → 60 57 → 60	0.11469 0.48106 0.49542	n→ π^* n→ π^* n→ π^*
S ₀ →S ₄	3.7649 eV/329.32 nm	0.1846	58 → 60 59 → 61	0.68108 0.14557	$\pi \rightarrow \pi^*, n \rightarrow \pi^*$ $\pi \rightarrow \pi^*, n \rightarrow \pi^*$
S ₀ →S ₅	4.1391 eV/299.54 nm	0.0000	54 → 60 57 → 60	0.68091 0.11805	n→ π^* n→ π^*
S ₀ →S ₆	4.2073 eV/294.69 nm	0.0121	55 → 60 59 → 61	0.68296 0.13590	$\pi \rightarrow \pi^*, n \rightarrow \pi^*$ $\pi \rightarrow \pi^*, n \rightarrow \pi^*$
S ₀ →S ₇	4.6715 eV/265.41 nm	0.0004	52 → 60 56 → 61	0.68362 0.13155	n→ π^* n→ π^*
S ₀ →S ₈	4.8343 eV/256.47 nm	0.0407	53 → 60 58 → 61	0.64940 0.23530	$\pi \rightarrow \pi^*, n \rightarrow \pi^*$ $\pi \rightarrow \pi^*, n \rightarrow \pi^*$
S ₀ →S ₉	4.8870 eV/253.70 nm	0.7327	55 → 60 58 → 60 59 → 61	0.15071 0.11478 0.65739	$\pi \rightarrow \pi^*, n \rightarrow \pi^*$ $\pi \rightarrow \pi^*, n \rightarrow \pi^*$ $\pi \rightarrow \pi^*, n \rightarrow \pi^*$
S ₀ →S ₁₀	5.2148 eV/237.75 nm	0.0003	52 → 60 56 → 61 57 → 61	0.12260 0.59739 0.33662	n→ π^* n→ π^* n→ π^*
S ₀ →T ₁	2.1524 eV/576.04 nm	0.0000	58 → 60 59 → 60	0.10512 0.69490	$\pi \rightarrow \pi^*, n \rightarrow \pi^*$ $\pi \rightarrow \pi^*, n \rightarrow \pi^*$
S ₀ →T ₂	2.7564 eV/449.80 nm	0.0000	58 → 60 58 → 62 59 → 60 59 → 61	0.65690 0.14210 0.10191 0.13926	$\pi \rightarrow \pi^*, n \rightarrow \pi^*$ $\pi \rightarrow \pi^*, n \rightarrow \pi^*$ $\pi \rightarrow \pi^*, n \rightarrow \pi^*$ $\pi \rightarrow \pi^*, n \rightarrow \pi^*$
S ₀ →T ₃	2.8757 eV/431.15 nm	0.0000	52 → 60 56 → 60 57 → 60	0.20097 0.59844 0.29162	n→ π^* n→ π^* n→ π^*
S ₀ →T ₄	3.2381 eV/382.90 nm	0.0000	54 → 60 56 → 60 57 → 60	0.17148 0.27731 0.60567	n→ π^* n→ π^* n→ π^*
S ₀ →T ₅	3.5826 eV/346.07 nm	0.0000	55 → 60 55 → 63 58 → 60 59 → 61	0.61066 0.12514 0.11312 0.27992	$\pi \rightarrow \pi^*, n \rightarrow \pi^*$ $\pi \rightarrow \pi^*, n \rightarrow \pi^*$ $\pi \rightarrow \pi^*, n \rightarrow \pi^*$ $\pi \rightarrow \pi^*, n \rightarrow \pi^*$

Table S5-2. Electronic transitions involved in the excitation of MB-FL.

MB-FL	Energy	f	Composition	CI	Character
$S_0 \rightarrow S_1$	2.9397 eV/421.76 nm	0.1266	$75 \rightarrow 77$	0.13109	$\pi \rightarrow \pi^*, n \rightarrow \pi^*$
			$76 \rightarrow 77$	0.68714	$\pi \rightarrow \pi^*, n \rightarrow \pi^*$
$S_0 \rightarrow S_2$	3.3054 eV/375.10 nm	0.0036	$73 \rightarrow 77$	0.49011	$n \rightarrow \pi^*$
			$74 \rightarrow 77$	0.49515	$n \rightarrow \pi^*$
$S_0 \rightarrow S_3$	3.4376 eV/360.67 nm	0.0678	$73 \rightarrow 77$	0.40367	$n \rightarrow \pi^*$
			$74 \rightarrow 77$	0.38758	$n \rightarrow \pi^*$
			$75 \rightarrow 77$	0.40088	$\pi \rightarrow \pi^*, n \rightarrow \pi^*$
$S_0 \rightarrow S_4$	3.4741 eV/356.88 nm	0.1751	$73 \rightarrow 77$	0.28775	$n \rightarrow \pi^*$
			$74 \rightarrow 77$	0.28474	$n \rightarrow \pi^*$
			$75 \rightarrow 77$	0.54711	$\pi \rightarrow \pi^*, n \rightarrow \pi^*$
			$76 \rightarrow 77$	0.10919	$\pi \rightarrow \pi^*, n \rightarrow \pi^*$
			$76 \rightarrow 78$	0.11555	$\pi \rightarrow \pi^*, n \rightarrow \pi^*$
$S_0 \rightarrow S_5$	4.1196 eV/300.97 nm	0.0004	$70 \rightarrow 77$	0.57012	$n \rightarrow \pi^*$
			$71 \rightarrow 77$	0.37398	$n \rightarrow \pi^*$
			$74 \rightarrow 77$	0.10777	$n \rightarrow \pi^*$
$S_0 \rightarrow S_6$	4.1836 eV/296.36 nm	0.0128	$72 \rightarrow 77$	0.67538	$n \rightarrow \pi^*$
			$76 \rightarrow 78$	0.15217	$n \rightarrow \pi^*$
$S_0 \rightarrow S_7$	4.3292 eV/286.39 nm	0.0014	$67 \rightarrow 77$	0.11551	$n \rightarrow \pi^*$
			$70 \rightarrow 77$	0.36602	$n \rightarrow \pi^*$
			$71 \rightarrow 77$	0.58022	$n \rightarrow \pi^*$
$S_0 \rightarrow S_8$	4.6399 eV/267.22 nm	0.3621	$68 \rightarrow 77$	0.15420	$\pi \rightarrow \pi^*, n \rightarrow \pi^*$
			$72 \rightarrow 77$	0.14294	$n \rightarrow \pi^*$
			$75 \rightarrow 78$	0.11895	$\pi \rightarrow \pi^*, n \rightarrow \pi^*$
			$75 \rightarrow 79$	0.11391	$\pi \rightarrow \pi^*, n \rightarrow \pi^*$
			$76 \rightarrow 78$	0.59254	$\pi \rightarrow \pi^*, n \rightarrow \pi^*$
			$76 \rightarrow 79$	0.17905	$\pi \rightarrow \pi^*, n \rightarrow \pi^*$
			$76 \rightarrow 80$	0.13154	$\pi \rightarrow \pi^*, n \rightarrow \pi^*$
$S_0 \rightarrow S_9$	4.6985 eV/263.88 nm	0.0289	$67 \rightarrow 77$	0.45904	$n \rightarrow \pi^*$
			$68 \rightarrow 77$	0.26507	$\pi \rightarrow \pi^*, n \rightarrow \pi^*$
			$69 \rightarrow 77$	0.30763	$\pi \rightarrow \pi^*, n \rightarrow \pi^*$
			$73 \rightarrow 78$	0.12149	$n \rightarrow \pi^*$
			$75 \rightarrow 78$	0.22353	$\pi \rightarrow \pi^*, n \rightarrow \pi^*$
			$76 \rightarrow 78$	0.14921	$\pi \rightarrow \pi^*, n \rightarrow \pi^*$
			$76 \rightarrow 79$	0.10128	$\pi \rightarrow \pi^*, n \rightarrow \pi^*$
$S_0 \rightarrow S_{10}$	4.7571 eV/260.63 nm	0.0106	$67 \rightarrow 77$	0.34442	$n \rightarrow \pi^*$
			$68 \rightarrow 77$	0.17458	$\pi \rightarrow \pi^*, n \rightarrow \pi^*$
			$69 \rightarrow 77$	0.39535	$\pi \rightarrow \pi^*, n \rightarrow \pi^*$
			$75 \rightarrow 78$	0.38672	$\pi \rightarrow \pi^*, n \rightarrow \pi^*$
			$76 \rightarrow 79$	0.12618	$\pi \rightarrow \pi^*, n \rightarrow \pi^*$
$S_0 \rightarrow T_1$	2.1377 eV/579.99 nm	0.0000	$75 \rightarrow 77$	0.20247	$\pi \rightarrow \pi^*, n \rightarrow \pi^*$
			$76 \rightarrow 77$	0.67195	$\pi \rightarrow \pi^*, n \rightarrow \pi^*$
$S_0 \rightarrow T_2$	2.5405 eV/488.03 nm	0.0000	$68 \rightarrow 77$	0.13567	$\pi \rightarrow \pi^*, n \rightarrow \pi^*$
			$75 \rightarrow 77$	0.63261	$\pi \rightarrow \pi^*, n \rightarrow \pi^*$

			$75 \rightarrow 79$	0.11344	$\pi \rightarrow \pi^*, n \rightarrow \pi^*$
			$76 \rightarrow 77$	0.19607	$\pi \rightarrow \pi^*, n \rightarrow \pi^*$
			$76 \rightarrow 78$	0.10225	$\pi \rightarrow \pi^*, n \rightarrow \pi^*$
$S_0 \rightarrow T_3$	2.8707 eV/431.89 nm	0.0000	$67 \rightarrow 77$	0.17473	$n \rightarrow \pi^*$
			$73 \rightarrow 77$	0.57454	$n \rightarrow \pi^*$
			$74 \rightarrow 77$	0.33942	$n \rightarrow \pi^*$
$S_0 \rightarrow T_4$	3.2265 eV/384.27 nm	0.0000	$70 \rightarrow 77$	0.15251	$n \rightarrow \pi^*$
			$73 \rightarrow 77$	0.32735	$n \rightarrow \pi^*$
			$74 \rightarrow 77$	0.58236	$n \rightarrow \pi^*$
$S_0 \rightarrow T_5$	3.5256 eV/351.66 nm	0.0000	$72 \rightarrow 77$	0.46177	$n \rightarrow \pi^*$
			$75 \rightarrow 77$	0.13015	$\pi \rightarrow \pi^*, n \rightarrow \pi^*$
			$75 \rightarrow 79$	0.10437	$\pi \rightarrow \pi^*, n \rightarrow \pi^*$
			$76 \rightarrow 78$	0.46178	$\pi \rightarrow \pi^*, n \rightarrow \pi^*$

Table S5-3. Electronic transitions involved in the excitation of DB-FL.

DB-FL	Energy	f	Composition	CI	Character
S ₀ →S ₁	2.9061 eV/426.64 nm	0.2562	93 → 94	0.69605	$\pi \rightarrow \pi^*, n \rightarrow \pi^*$
S ₀ →S ₂	3.2895 eV/376.91 nm	0.0007	90 → 94 91 → 94	0.45975 0.52471	n→ π^* n→ π^*
S ₀ →S ₃	3.4127 eV/363.31 nm	0.0001	86 → 94 90 → 94 91 → 94	0.10528 0.52556 0.44948	n→ π^* n→ π^* n→ π^*
S ₀ →S ₄	3.6065 eV/343.78 nm	0.2527	92 → 94 93 → 95	0.68436 0.12714	$\pi \rightarrow \pi^*, n \rightarrow \pi^*$ $\pi \rightarrow \pi^*, n \rightarrow \pi^*$
S ₀ →S ₅	4.0742 eV/304.32 nm	0.0000	86 → 94 88 → 94 91 → 94	0.62883 0.27001 0.11108	n→ π^* n→ π^* n→ π^*
S ₀ →S ₆	4.0924 eV/302.96 nm	0.0057	87 → 94 89 → 94	0.52915 0.45640	n→ π^* $\pi \rightarrow \pi^*, n \rightarrow \pi^*$
S ₀ →S ₇	4.1394 eV/299.52 nm	0.0000	86 → 94 88 → 94	0.26423 0.65064	n→ π^* n→ π^*
S ₀ →S ₈	4.1701 eV/297.32 nm	0.0153	87 → 94 89 → 94 93 → 95	0.43540 0.51342 0.16501	n→ π^* $\pi \rightarrow \pi^*, n \rightarrow \pi^*$ $\pi \rightarrow \pi^*, n \rightarrow \pi^*$
S ₀ →S ₉	4.5884 eV/270.21 nm	0.0000	89 → 96 93 → 96	0.13368 0.69182	$\pi \rightarrow \pi^*, n \rightarrow \pi^*$ $\pi \rightarrow \pi^*, n \rightarrow \pi^*$
S ₀ →S ₁₀	4.6606 eV/266.03 nm	0.0004	83 → 94 85 → 94 90 → 95	0.65622 0.18944 0.13568	n→ π^* n→ π^* n→ π^*
S ₀ →T ₁	2.0857 eV/594.45 nm	0.0000	93 → 94	0.69106	$\pi \rightarrow \pi^*, n \rightarrow \pi^*$
S ₀ →T ₂	2.6797 eV/462.67 nm	0.0000	84 → 94 92 → 94 92 → 97 93 → 95	0.14042 0.64343 0.13561 0.15148	$\pi \rightarrow \pi^*, n \rightarrow \pi^*$ $\pi \rightarrow \pi^*, n \rightarrow \pi^*$ $\pi \rightarrow \pi^*, n \rightarrow \pi^*$ $\pi \rightarrow \pi^*, n \rightarrow \pi^*$
S ₀ →T ₃	2.8770 eV/430.95 nm	0.0000	83 → 94 90 → 94 91 → 94	0.19213 0.59319 0.30431	n→ π^* n→ π^* n→ π^*
S ₀ →T ₄	3.1872 eV/389.00 nm	0.0000	86 → 94 90 → 94 91 → 94	0.16812 0.29058 0.59944	n→ π^* n→ π^* n→ π^*
S ₀ →T ₅	3.4906 eV/355.20 nm	0.0000	87 → 94 89 → 94 92 → 94 93 → 95	0.40901 0.32527 0.11877 0.42272	n→ π^* $\pi \rightarrow \pi^*, n \rightarrow \pi^*$ $\pi \rightarrow \pi^*, n \rightarrow \pi^*$ $\pi \rightarrow \pi^*, n \rightarrow \pi^*$

Table S5-4. Electronic transitions involved in the excitation of Ph-FL.

Ph-FL	Energy	f	Composition	CI	Character
S ₀ →S ₁	3.0223 eV/410.23 nm	0.2141	75 → 76	0.69440	$\pi \rightarrow \pi^*, n \rightarrow \pi^*$
S ₀ →S ₂	3.2805 eV/377.94 nm	0.0006	70 → 76	0.38996	$\pi \rightarrow \pi^*, n \rightarrow \pi^*$
			72 → 76	0.45592	n→π*
			74 → 76	0.36410	$\pi \rightarrow \pi^*, n \rightarrow \pi^*$
S ₀ →S ₃	3.3792 eV/366.91 nm	0.0000	68 → 76	0.11760	n→π*
			72 → 76	0.47665	$\pi \rightarrow \pi^*, n \rightarrow \pi^*$
			74 → 76	0.49177	$\pi \rightarrow \pi^*, n \rightarrow \pi^*$
S ₀ →S ₄	3.6278 eV/341.76 nm	0.0818	73 → 76	0.69305	$\pi \rightarrow \pi^*, n \rightarrow \pi^*$
S ₀ →S ₅	3.7189 eV/333.39 nm	0.0003	70 → 76	0.56842	$\pi \rightarrow \pi^*, n \rightarrow \pi^*$
			72 → 76	0.22251	n→π*
			74 → 76	0.34254	$\pi \rightarrow \pi^*, n \rightarrow \pi^*$
S ₀ →S ₆	3.7974 eV/326.50 nm	0.1195	71 → 76	0.68816	$\pi \rightarrow \pi^*, n \rightarrow \pi^*$
			75 → 77	0.11349	$\pi \rightarrow \pi^*, n \rightarrow \pi^*$
S ₀ →S ₇	4.1396 eV/299.51 nm	0.0000	68 → 76	0.67877	n→π*
S ₀ →S ₈	4.1978 eV/295.35 nm	0.0131	69 → 76	0.68349	n→π*
			75 → 77	0.13401	$\pi \rightarrow \pi^*, n \rightarrow \pi^*$
S ₀ →S ₉	4.6988 eV/263.87 nm	0.0002	66 → 76	0.67118	$\pi \rightarrow \pi^*, n \rightarrow \pi^*$
			70 → 77	0.10706	$\pi \rightarrow \pi^*, n \rightarrow \pi^*$
			74 → 77	0.10839	$\pi \rightarrow \pi^*, n \rightarrow \pi^*$
S ₀ →S ₁₀	4.8520 eV/255.53 nm	0.2252	67 → 76	0.56461	$\pi \rightarrow \pi^*, n \rightarrow \pi^*$
			71 → 77	0.13175	$\pi \rightarrow \pi^*, n \rightarrow \pi^*$
			73 → 77	0.17685	$\pi \rightarrow \pi^*, n \rightarrow \pi^*$
			75 → 77	0.33909	$\pi \rightarrow \pi^*, n \rightarrow \pi^*$
S ₀ →T ₁	2.1429 eV/578.58 nm	0.0000	75 → 76	0.69244	$\pi \rightarrow \pi^*, n \rightarrow \pi^*$
S ₀ →T ₂	2.7509 eV/450.71 nm	0.0000	71 → 76	0.43977	$\pi \rightarrow \pi^*, n \rightarrow \pi^*$
			73 → 76	0.48775	$\pi \rightarrow \pi^*, n \rightarrow \pi^*$
			75 → 76	0.11713	$\pi \rightarrow \pi^*, n \rightarrow \pi^*$
			75 → 77	0.12672	$\pi \rightarrow \pi^*, n \rightarrow \pi^*$
S ₀ →T ₃	2.8421 eV/436.25 nm	0.0000	66 → 76	0.18655	$\pi \rightarrow \pi^*, n \rightarrow \pi^*$
			70 → 76	0.47385	$\pi \rightarrow \pi^*, n \rightarrow \pi^*$
			72 → 76	0.39268	n→π*
			74 → 76	0.26266	$\pi \rightarrow \pi^*, n \rightarrow \pi^*$
S ₀ →T ₄	3.1972 eV/387.79 nm	0.0000	68 → 76	0.17012	n→π*
			70 → 76	0.15968	$\pi \rightarrow \pi^*, n \rightarrow \pi^*$
			72 → 76	0.49924	n→π*
			74 → 76	0.41784	$\pi \rightarrow \pi^*, n \rightarrow \pi^*$
S ₀ →T ₅	3.5620 eV/348.08 nm	0.0000	69 → 76	0.59168	n→π*
			69 → 81	0.12104	n→π*
			73 → 76	0.16351	$\pi \rightarrow \pi^*, n \rightarrow \pi^*$
			75 → 77	0.29034	$\pi \rightarrow \pi^*, n \rightarrow \pi^*$

Table S5-5. Electronic transitions involved in the excitation of DB-FL calculated at CAM-B3LYP/6-311G(d) level of theory.

DB-FL	Energy	f	Composition	CI	Character
S ₀ →S ₁	3.3450 eV/370.65 nm	0.4102	93 → 94	0.69392	$\pi \rightarrow \pi^*, n \rightarrow \pi^*$
S ₀ →S ₂	3.7020 eV/334.92 nm	0.0014	83 → 94 90 → 94 91 → 94	0.17031 0.54959 0.37803	n→ π^* n→ π^* n→ π^*
S ₀ →S ₃	4.1409 eV/299.42 nm	0.0000	86 → 94 86 → 98 90 → 94 91 → 94 91 → 98	0.27013 0.10753 0.34727 0.49646 0.12821	n→ π^* n→ π^* n→ π^* n→ π^* n→ π^*
S ₀ →S ₄	4.2374 eV/292.59 nm	0.2240	92 → 94 93 → 95	0.67046 0.15901	$\pi \rightarrow \pi^*, n \rightarrow \pi^*$ $\pi \rightarrow \pi^*, n \rightarrow \pi^*$
S ₀ →S ₅	4.8750 eV/254.32 nm	0.1365	82 → 94 87 → 94 89 → 94 92 → 95 93 → 95 93 → 97	0.12842 0.47370 0.28411 0.13935 0.34286 0.14371	$\pi \rightarrow \pi^*, n \rightarrow \pi^*$ n→ π^* $\pi \rightarrow \pi^*, n \rightarrow \pi^*$ $\pi \rightarrow \pi^*, n \rightarrow \pi^*$ $\pi \rightarrow \pi^*, n \rightarrow \pi^*$ $\pi \rightarrow \pi^*, n \rightarrow \pi^*$
S ₀ →S ₆	4.9859 eV/248.67 nm	0.0000	83 → 94 86 → 94 86 → 100 90 → 94 90 → 95 91 → 94 91 → 95 91 → 100	0.22099 0.51583 0.10783 0.16092 0.13439 0.20102 0.16261 0.10466	n→ π^* n→ π^* n→ π^* n→ π^* n→ π^* n→ π^* n→ π^* n→ π^*
S ₀ →S ₇	5.1049 eV/242.87 nm	0.4649	89 → 94 92 → 94 92 → 95 93 → 95 93 → 97	0.41954 0.18163 0.11627 0.46674 0.17089	$\pi \rightarrow \pi^*, n \rightarrow \pi^*$ $\pi \rightarrow \pi^*, n \rightarrow \pi^*$
S ₀ →S ₈	5.1560 eV/240.47 nm	0.0001	83 → 94 86 → 94 90 → 95 90 → 98 91 → 94 91 → 95	0.54052 0.20740 0.24472 0.11480 0.10575 0.14850	n→ π^* n→ π^* n→ π^* n→ π^* n→ π^* n→ π^*
S ₀ →S ₉	5.1879 eV/238.99 nm	0.5425	87 → 94 89 → 94 92 → 95 93 → 95 93 → 97	0.50182 0.29694 0.14696 0.32555 0.10585	n→ π^* $\pi \rightarrow \pi^*, n \rightarrow \pi^*$ $\pi \rightarrow \pi^*, n \rightarrow \pi^*$ $\pi \rightarrow \pi^*, n \rightarrow \pi^*$ $\pi \rightarrow \pi^*, n \rightarrow \pi^*$

$S_0 \rightarrow S_{10}$	5.2890 eV/234.42 nm	0.0001	89 → 94 93 → 96	0.31195 0.61391	$\pi \rightarrow \pi^*, n \rightarrow \pi^*$ $\pi \rightarrow \pi^*, n \rightarrow \pi^*$
$S_0 \rightarrow T_1$	2.2529 eV/550.32 nm	0.0000	89 → 94 92 → 94 93 → 94	0.12909 0.19278 0.64457	$\pi \rightarrow \pi^*, n \rightarrow \pi^*$ $\pi \rightarrow \pi^*, n \rightarrow \pi^*$ $\pi \rightarrow \pi^*, n \rightarrow \pi^*$
$S_0 \rightarrow T_2$	2.8423 eV/436.21 nm	0.0000	84 → 94 92 → 94 92 → 97 93 → 94 93 → 95	0.16780 0.53188 0.20812 0.20711 0.27116	$\pi \rightarrow \pi^*, n \rightarrow \pi^*$ $\pi \rightarrow \pi^*, n \rightarrow \pi^*$
$S_0 \rightarrow T_3$	3.1216 eV/397.18 nm	0.0000	83 → 94 90 → 94 91 → 94	0.26676 0.52929 0.32157	$n \rightarrow \pi^*$ $n \rightarrow \pi^*$ $n \rightarrow \pi^*$
$S_0 \rightarrow T_4$	3.7751 eV/328.42 nm	0.0000	89 → 94 92 → 94 93 → 94 93 → 95	0.22791 0.26179 0.10752 0.55719	$\pi \rightarrow \pi^*, n \rightarrow \pi^*$ $\pi \rightarrow \pi^*, n \rightarrow \pi^*$ $\pi \rightarrow \pi^*, n \rightarrow \pi^*$ $\pi \rightarrow \pi^*, n \rightarrow \pi^*$
$S_0 \rightarrow T_5$	3.8117 eV/325.27 nm	0.0000	86 → 94 86 → 98 90 → 94 91 → 94 91 → 98	0.29286 0.14513 0.26990 0.49905 0.16704	$n \rightarrow \pi^*$ $n \rightarrow \pi^*$ $n \rightarrow \pi^*$ $n \rightarrow \pi^*$ $n \rightarrow \pi^*$

Table S5-6. Electronic transitions involved in the excitation of DB-FL calculated at ωB97XD/6-311G(d) level of theory.

DB-FL	Energy	f	Composition	CI	Character
S ₀ →S ₁	3.3367 eV/371.58 nm	0.4101	93 → 94	0.69084	$\pi \rightarrow \pi^*, n \rightarrow \pi^*$
S ₀ →S ₂	3.6665 eV/338.15 nm	0.0013	83 → 94 90 → 94 91 → 94	0.16729 0.57318 0.34299	n→π* n→π* n→π*
S ₀ →S ₃	4.1161 eV/301.22 nm	0.0000	86 → 94 86 → 98 90 → 94 91 → 94 91 → 98	0.28907 0.10694 0.31115 0.50901 0.12887	n→π* n→π* n→π* n→π* n→π*
S ₀ →S ₄	4.2646 eV/290.73 nm	0.2252	84 → 98 92 → 94 93 → 95	0.10718 0.66427 0.16150	$\pi \rightarrow \pi^*, n \rightarrow \pi^*$ $\pi \rightarrow \pi^*, n \rightarrow \pi^*$ $\pi \rightarrow \pi^*, n \rightarrow \pi^*$
S ₀ →S ₅	4.8725 eV/254.46 nm	0.1149	82 → 94 87 → 94 89 → 94 92 → 95 93 → 95 93 → 97	0.14158 0.48250 0.26198 0.15153 0.32597 0.16293	$\pi \rightarrow \pi^*, n \rightarrow \pi^*$ n→π* $\pi \rightarrow \pi^*, n \rightarrow \pi^*$ $\pi \rightarrow \pi^*, n \rightarrow \pi^*$ $\pi \rightarrow \pi^*, n \rightarrow \pi^*$ $\pi \rightarrow \pi^*, n \rightarrow \pi^*$
S ₀ →S ₆	5.0009 eV/247.92 nm	0.0001	83 → 94 86 → 94 90 → 94 90 → 95 91 → 94 91 → 95 91 → 100	0.29281 0.47262 0.16543 0.15741 0.20459 0.15122 0.10478	n→π* n→π* n→π* n→π* n→π* n→π* n→π*
S ₀ →S ₇	5.1294 eV/241.71 nm	0.5358	89 → 94 92 → 94 92 → 95 93 → 95 93 → 97	0.36396 0.19281 0.12203 0.48566 0.20350	$\pi \rightarrow \pi^*, n \rightarrow \pi^*$ $\pi \rightarrow \pi^*, n \rightarrow \pi^*$
S ₀ →S ₈	5.1507 eV/240.71 nm	0.0001	83 → 94 86 → 94 90 → 95 90 → 98 91 → 94 91 → 95	0.50632 0.26909 0.23037 0.11020 0.13372 0.15959	n→π* n→π* n→π* n→π* n→π* n→π*
S ₀ →S ₉	5.2000 eV/238.43 nm	0.5084	87 → 94 89 → 94 92 → 95 93 → 95 93 → 97	0.48516 0.31279 0.16389 0.30926 0.13271	n→π* $\pi \rightarrow \pi^*, n \rightarrow \pi^*$ $\pi \rightarrow \pi^*, n \rightarrow \pi^*$ $\pi \rightarrow \pi^*, n \rightarrow \pi^*$ $\pi \rightarrow \pi^*, n \rightarrow \pi^*$

$S_0 \rightarrow S_{10}$	5.3921 eV/229.94 nm	0.0001	$89 \rightarrow 96$ $93 \rightarrow 96$	0.34049 0.59605	$\pi \rightarrow \pi^*, n \rightarrow \pi^*$ $\pi \rightarrow \pi^*, n \rightarrow \pi^*$
$S_0 \rightarrow T_1$	2.2860 eV/542.37 nm	0.0000	$89 \rightarrow 94$ $92 \rightarrow 94$ $93 \rightarrow 94$	0.13161 0.16136 0.65347	$\pi \rightarrow \pi^*, n \rightarrow \pi^*$ $\pi \rightarrow \pi^*, n \rightarrow \pi^*$ $\pi \rightarrow \pi^*, n \rightarrow \pi^*$
$S_0 \rightarrow T_2$	2.9297 eV/423.19 nm	0.0000	$84 \rightarrow 94$ $92 \rightarrow 94$ $92 \rightarrow 97$ $93 \rightarrow 94$ $93 \rightarrow 95$	0.17652 0.54959 0.20292 0.17391 0.25630	$\pi \rightarrow \pi^*, n \rightarrow \pi^*$ $\pi \rightarrow \pi^*, n \rightarrow \pi^*$
$S_0 \rightarrow T_3$	3.1354 eV/395.44 nm	0.0000	$83 \rightarrow 94$ $90 \rightarrow 94$ $90 \rightarrow 97$ $91 \rightarrow 94$	0.25735 0.55100 0.10185 0.29505	$n \rightarrow \pi^*$ $n \rightarrow \pi^*$ $n \rightarrow \pi^*$ $n \rightarrow \pi^*$
$S_0 \rightarrow T_4$	3.8120 eV/325.25 nm	0.0000	$86 \rightarrow 94$ $86 \rightarrow 98$ $90 \rightarrow 94$ $91 \rightarrow 94$ $91 \rightarrow 97$ $91 \rightarrow 98$	0.30763 0.14162 0.24253 0.50691 0.10150 0.16529	$n \rightarrow \pi^*$ $n \rightarrow \pi^*$ $n \rightarrow \pi^*$ $n \rightarrow \pi^*$ $n \rightarrow \pi^*$ $, n \rightarrow \pi^*$
$S_0 \rightarrow T_5$	3.8272 eV/323.96 nm	0.0000	$89 \rightarrow 94$ $92 \rightarrow 98$ $93 \rightarrow 95$	0.23036 0.24300 0.56472	$\pi \rightarrow \pi^*, n \rightarrow \pi^*$ $\pi \rightarrow \pi^*, n \rightarrow \pi^*$ $\pi \rightarrow \pi^*, n \rightarrow \pi^*$

Table S5-7. Calculated spin-orbit coupling matrix elements of FLPSs (cm^{-1}), between the emitting states and the perturbing states with different multiplicity, calculated as

$$\sqrt{\left(\left|\langle S_0 | H^{SO} | T_{1,x} \rangle\right|^2 + \left|\langle S_0 | H^{SO} | T_{1,y} \rangle\right|^2 + \left|\langle S_0 | H^{SO} | T_{1,z} \rangle\right|^2\right)/3} .$$

FLPSs	FL	MB-FL	DB-FL	Ph-FL
$S_1 \rightarrow T_1$	1.27×10^{-3}	4.01	0.26	4.84
$T_1 \rightarrow S_0$	0.27	4.59	0.0056	0.36

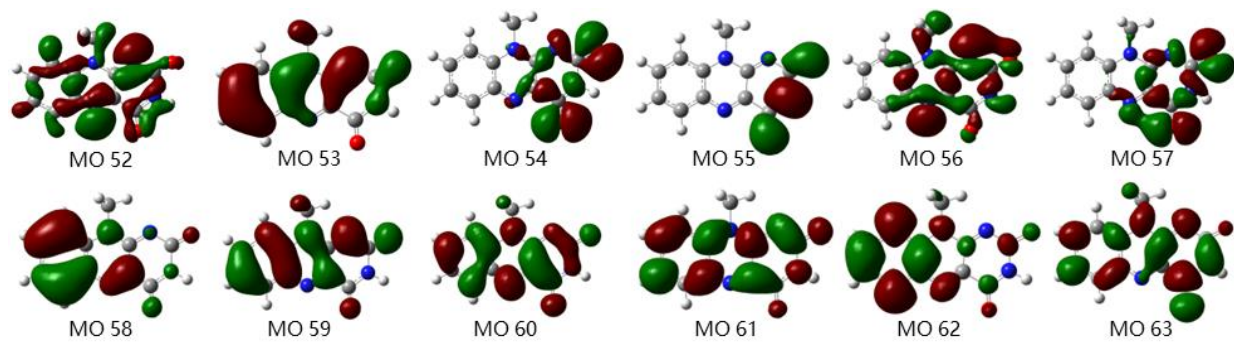


Figure S5-1. Isosurface plots of frontier molecular orbitals of FL involved in electron transitions contribute to UV-vis absorption. (Isovalue: ± 0.02 a.u.; C: Gray; O: Red; N: Blue; H: White.)

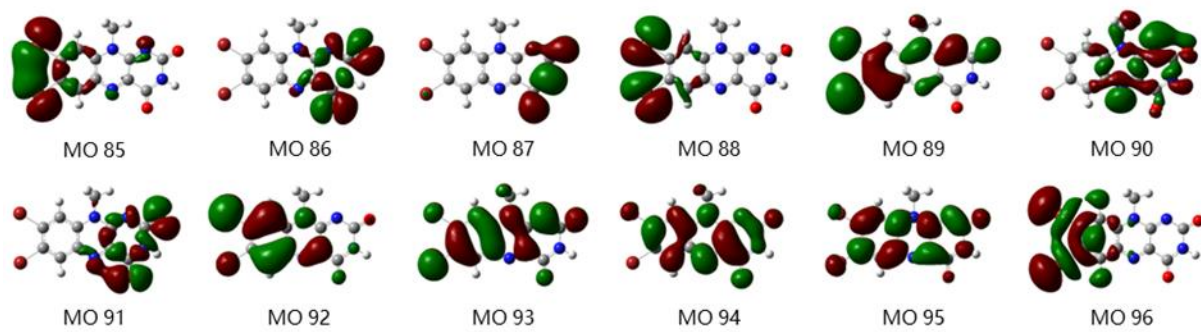


Figure S5-2. Isosurface plots of frontier molecular orbitals of DB-FL involved in electron transitions contribute to UV-vis absorption. (Isovalue: ± 0.02 a.u.; C: Gray; O: Red; N: Blue; H: White.)

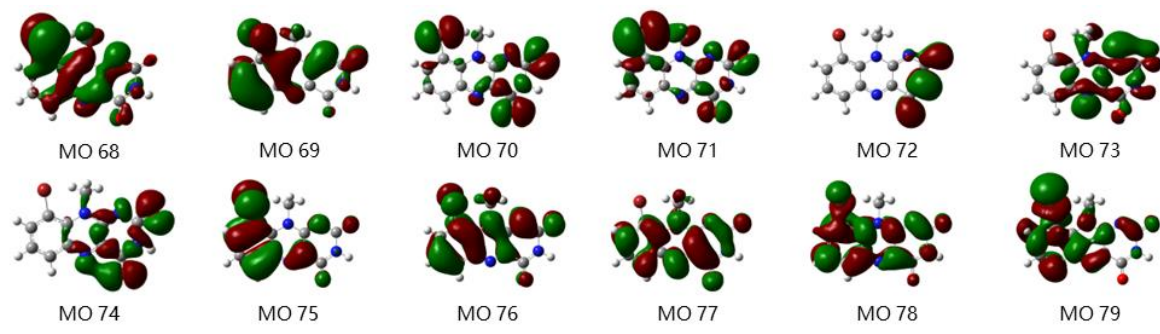


Figure S5-3. Isosurface plots of frontier molecular orbitals of MB-FL involved in electron transitions contribute to UV-vis absorption. (Isovalue: ± 0.02 a.u.; C: Gray; O: Red; N: Blue; H: White.)

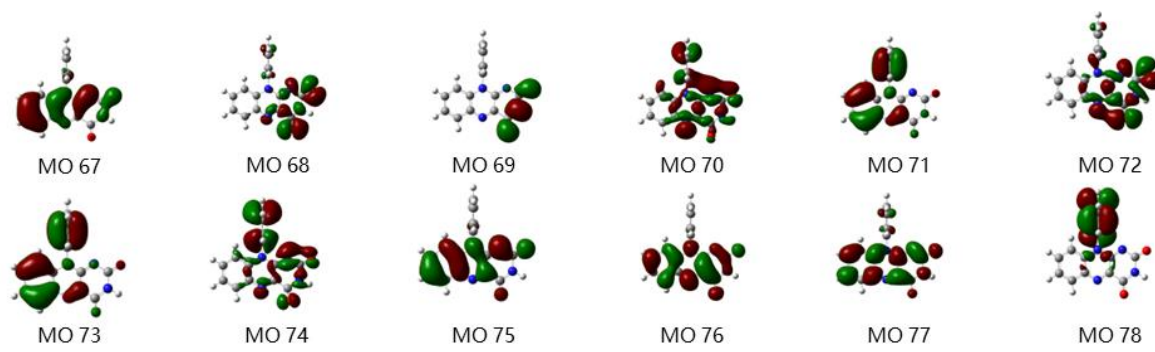


Figure S5-4. Isosurface plots of frontier molecular orbitals of Ph-FL involved in electron transitions contribute to UV-vis absorption. (Isovalue: ± 0.02 a.u.; C: Gray; O: Red; N: Blue; H: White.)

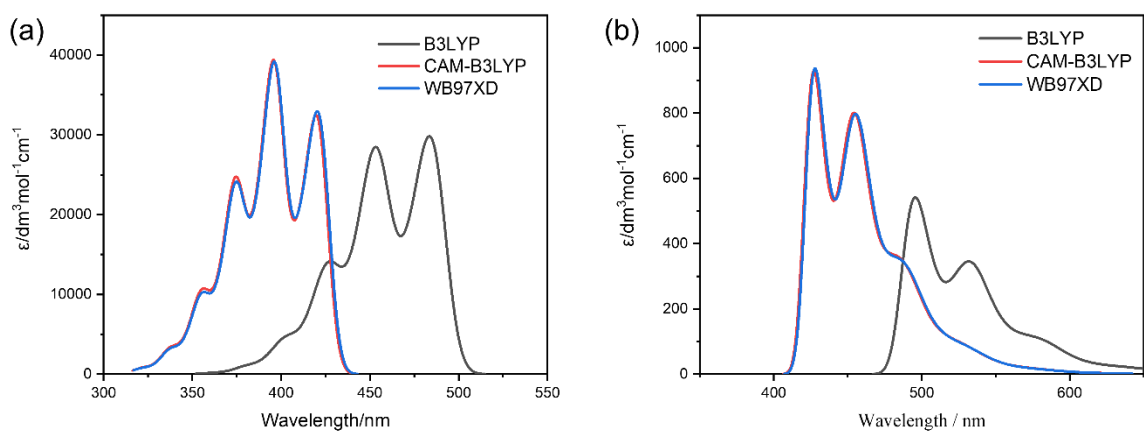


Figure S5-5 The vibration resolved absorption(a) and emission (b) spectra of DB-FL calculated with B3LYP, CAM-B3LYP and ω B97XD functionals.

6. References

1. R. C. Binning and L. A. Curtiss, *J. Comput. Chem.*, 1990, **11**, 1206-1216.
2. M. M. Franci, W. J. Pietro, W. J. Hehre, J. S. Binkley, M. S. Gordon, D. J. Defrees and J. A. Pople, *J. Chem. Phys.*, 1982, **77**, 3654-3665.
3. V. A. Rassolov, M. A. Ratner, J. A. Pople, P. C. Redfern and L. A. Curtiss, *J. Comput. Chem.*, 2001, **22**, 976-984.
4. A. D. Becke, *J. Chem. Phys.*, 1993, **98**, 5648-5652.
5. C. T. Lee, W. T. Yang and R. G. Parr, *Phys. Rev. B*, 1988, **37**, 785-789.
6. S. Miertus, E. Scrocco and J. Tomasi, *Chem. Phys.*, 1981, **55**, 117-129.
7. R. Cammi and B. Mennucci, *J. Chem. Phys.*, 1999, **110**, 9877-9886.
8. J. Tomasi, B. Mennucci and R. Cammi, *Chem. Rev.*, 2005, **105**, 2999-3093.
9. M. J. Frisch, G. W. Trucks, H. B. Schlegel, G. E. Scuseria, M. A. Robb, J. R. Cheeseman, G. Scalmani, V. Barone, G. A. Petersson, H. Nakatsuji, X. Li, M. Caricato, A. V. Marenich, J. Bloino, B. G. Janesko, R. Gomperts, B. Mennucci, H. P. Hratchian, J. V. Ortiz, A. F. Izmaylov, J. L. Sonnenberg, Williams, F. Ding, F. Lipparini, F. Egidi, J. Goings, B. Peng, A. Petrone, T. Henderson, D. Ranasinghe, V. G. Zakrzewski, J. Gao, N. Rega, G. Zheng, W. Liang, M. Hada, M. Ehara, K. Toyota, R. Fukuda, J. Hasegawa, M. Ishida, T. Nakajima, Y. Honda, O. Kitao, H. Nakai, T. Vreven, K. Throssell, J. A. Montgomery Jr., J. E. Peralta, F. Ogliaro, M. J. Bearpark, J. J. Heyd, E. N. Brothers, K. N. Kudin, V. N. Staroverov, T. A. Keith, R. Kobayashi, J. Normand, K. Raghavachari, A. P. Rendell, J. C. Burant, S. S. Iyengar, J. Tomasi, M. Cossi, J. M. Millam, M. Klene, C. Adamo, R. Cammi, J. W. Ochterski, R. L. Martin, K. Morokuma, O. Farkas, J. B. Foresman and D. J. Fox, *Journal*, 2016.
10. O. Vahtras, H. Agren, P. Jorgensen, H. J. A. Jensen, T. Helgaker and J. Olsen, *J. Chem. Phys.*, 1992, **97**, 9178-9187.
11. H. Hettema, H. J. A. Jensen, P. Jorgensen and J. Olsen, *J. Chem. Phys.*, 1992, **97**, 1174-1190.
12. H. Agren, O. Vahtras, H. Koch, P. Jorgensen and T. Helgaker, *J. Chem. Phys.*, 1993, **98**, 6417-6423.
13. J. Olsen, D. L. Yeager and P. Jorgensen, *J. Chem. Phys.*, 1989, **91**, 381-388.
14. P. Jorgensen, H. J. A. Jensen and J. Olsen, *J. Chem. Phys.*, 1988, **89**, 3654-3661.
15. K. Aidan, C. Angeli, K. L. Bak, V. Bakken, R. Bast, L. Boman, O. Christiansen, R. Cimiraglia, S. Coriani, P. Dahle, E. K. Dalskov, U. Ekstrom, T. Enevoldsen, J. J. Eriksen, P. Ettenhuber, B. Fernandez, L. Ferrighi, H. Fliegl, L. Frediani, K. Hald, A. Halkier, C. Hattig, H. Heiberg, T. Helgaker, A. C. Hennum, H. Hettema, E. Hjertenes, S. Host, I. M. Hoyvik, M. F. Iozzi, B. Jansik, H. J. A. Jensen, D. Jonsson, P. Jorgensen, J. Kauczor, S. Kirpekar, T. Kjrgaard, W. Klopper, S. Knecht, R. Kobayashi, H. Koch, J. Kongsted, A. Krapp, K. Kristensen, A. Ligabue, O. B. Lutnaes, J. I. Melo, K. V. Mikkelsen, R. H. Myhre, C. Neiss, C. B. Nielsen, P. Norman, J. Olsen, J. M. H. Olsen, A. Osted, M. J. Packer, F. Pawlowski, T. B. Pedersen, P. F. Provasi, S. Reine, Z. Rinkevicius, T. A. Ruden, K. Ruud, V. V. Rybkin, P. Salek, C. C. M. Samson, A. S. de Meras, T. Saue, S. P. A. Sauer, B. Schimmelpfennig, K. Sneskov, A. H. Steindal, K. O. Sylvester-Hvid, P. R. Taylor, A. M. Teale, E. I. Tellgren, D. P. Tew, A. J. Thorvaldsen, L. Thogersen, O. Vahtras, M. A. Watson, D. J. D. Wilson, M. Ziolkowski and H. Agren, *Wiley Interdiscip. Rev.-Comput. Mol. Sci.*, 2014, **4**, 269-284.

16. Q. Peng, Y. P. Yi, Z. G. Shuai and J. S. Shao, *J. Chem. Phys.*, 2007, **126**, 114302.
17. Q. Peng, Y. P. Yi, Z. G. Shuai and J. S. Shao, *J. Am. Chem. Soc.*, 2007, **129**, 9333-9339.
18. Y. L. Niu, Q. A. Peng, C. M. Deng, X. Gao and Z. G. Shuai, *J. Phys. Chem. A*, 2010, **114**, 7817-7831.
19. Y. Niu, Q. Peng and Z. Shuai, *Sci. China Ser. B-Chem.*, 2008, **51**, 1153-1158.
20. Q. Peng, Y. L. Niu, Q. H. Shi, X. Gao and Z. G. Shuai, *J. Chem. Theory Comput.*, 2013, **9**, 1132-1143.